Quaternary Science Reviews 184 (2018) 5–25

Contents lists available at ScienceDirect

Quaternary Science Reviews

journal homepage: www.elsevier.com/locate/quascirev

Dating human occupation and adaptation in the southern European last glacial refuge: The chronostratigraphy of Grotta del Romito (Italy)

Simon Blockley [a, *], Maura Pellegrini [b], Andre C. Colonese [c], Domenico Lo Vetro [d, e], Paul G. Albert [b], Achim Brauer [c], Zelia Di Giuseppe [f], Adrian Evans [f], Poppy Harding [h], Julia Lee-Thorp [b], Paul Lincoln [a], Fabio Martini [d, e], Mark Pollard [b], Victoria Smith [b], Randolph Donahue [g]

[a] Centre for Quaternary Research, Royal Holloway, University of London, Egham Hill, Surrey, TW20 0EX, UK
[b] Research Laboratory for Archaeology and the History of Art, University of Oxford, Dyson Perrins Building, South Parks Road, Oxford, OX1 3QY, UK
[c] BioArCh, Department of Archaeology, University of York, Biology S. Block, Wentworth Way, York, YO10 5DD, UK
[d] Archeologia Preistorica, Dipartimento di Storia, Archeologia, Geografia, Arte e Spettacolo (SAGAS), Università degli Studi di Firenze, Via S. Egidio 21, 50122, Firenze, Italy
[e] Museo e Istituto Fiorentino di Preistoria, Via S. Egidio 21, 50122, Firenze, Italy
[f] GFZ German Research Centre for Geosciences, Section 5.2 Climate Dynamics and Landscape Evolution, 14473 Potsdam, Germany
[g] School of Archaeological Sciences, University of Bradford, Bradford, BD7 1DP, UK
[h] Environmental Change Research Centre, Department of Geography, UCL, Gower Street, London, WC1E 6BT, UK

ARTICLE INFO

Article history:
Received 27 January 2017
Received in revised form
12 September 2017
Accepted 18 September 2017
Available online 8 October 2017

Keywords:
Italian Peninsula
Upper Palaeolithic Dispersal
Cave deposit
Radiocarbon dating
Bayesian age model
Tephrochronology

ABSTRACT

Grotta del Romito has been the subject of numerous archaeological, chronological and palaeoenvironmental investigations for more than a decade. During the Upper Palaeolithic period the site contains evidence of human occupation through the Gravettian and Epigravettian periods, multiple human burials, changes in the pattern of human occupation, and faunal, isotopic and sedimentological evidence for local environmental change. In spite of this rich record, the chronological control is insufficient to resolve shifts in subsistence and mobility patterns at sufficiently high resolution to match the abrupt climate fluctuations at this time. To resolve this we present new radiocarbon and tephrostratigraphic dates in combination with existing radiocarbon dates, and develop a Bayesian age model framework for the site. This improved chronology reveals that local environmental conditions reflect abrupt and long-term changes in climate, and that these also directly influence changing patterns of human occupation of the site. In particular, we show that the environmental record for the site, based on small mammal habitat preferences, is chronologically in phase with the main changes in climate and environment seen in key regional archives from Italy and Greenland. We also calculate the timing of the transitions between different cultural phases and their spans. We also show that the intensification in occupation of the site is chronologically coincident with a rapid rise in Mesic Woody taxa seen in key regional pollen records and is associated with the Late Epigravettian occupation of the site. This change in the record of Grotta del Romito is also closely associated stratigraphically with a new tephra (the ROM-D30 tephra), which may act as a critical marker in environmental records of the region.

© 2017 Elsevier Ltd. All rights reserved.

1. Introduction

Glacial refugia are key geographic areas for understanding long-term human and biological responses to Late Pleistocene climate variability in Europe (Gamble et al., 2004, 2005; Willis and Whittaker, 2000). It is now widely accepted that large parts of the European population, as well as many species of animals and plants, were contracted to southern areas of the subcontinent around the Last Glacial Maximum, or more strictly Greenland Stadial 2 at 27–19 ky ago (Gamble et al., 2004, 2005; Willis and Whittaker, 2000; Bocquet-Appel et al., 2005; Torroni et al., 2001; Brewster et al., 2014; Fu et al., 2016; Posth et al., 2016; Rasmussen et al., 2006, 2014). Southwest France and the Iberian and Italian

* Corresponding author.
E-mail address: simon.blockley@rhul.ac.uk (S. Blockley).

https://doi.org/10.1016/j.quascirev.2017.09.007
0277-3791/© 2017 Elsevier Ltd. All rights reserved.

Peninsulas were critical areas for human population and biological concentration and sources of postglacial expansion to northern and central areas of Europe (Sommer and Nadachowski, 2006; Torroni et al., 2001; Brewster et al., 2014; Tallavaara et al., 2015; Fu et al., 2016; Posth et al., 2016). However, given the variability of climate conditions in southern Europe during the Lateglacial (Strandberg et al., 2011), as well as the complexity of archaeological and genetic records (e.g. Tallavaara et al., 2015), correlations between demographic, cultural and genetic evidence are not straightforward. A thorough understanding of the impact of Late Pleistocene environmental changes on European populations require robust *intra-situ* chronological frameworks to link climate events - often derived from highly resolved environmental archives - with archaeological records essentially preserved in sedimentary deposits in rock-shelters and caves. These are by far the most widely accessed sources of material culture and biological information for understanding trends and patterns in Late Pleistocene human-environment interaction in Southern Europe and Mediterranean areas (Woodward and Goldberg, 2001). However, the complex and discontinuous nature of archaeological and environmental deposits in caves, and the imprecision of individual calibrated ^{14}C ages, require the application of statistical methods for constraining the time of cultural and environmental events within such archives, in relation to regional records (Bronk Ramsey 2009a,b).

While models of hunter gatherer occupation of southern Europe have existed for many years it is only recently, with the significant advance in our understanding of the impact of abrupt climate change on Southern, as well as Northern Europe, that archaeologists are attempting to test these models against records of abrupt regional climate change. Pellegrini et al. (2008), for example, proposed to evaluate Higgs's (Higgs and Jarman, 1975) model of hunter-gatherer transhumance in Mediterranean Europe during the Lateglacial. Their aim was to test if the principal resources of the hunter-gatherers, red deer according to Higgs and Steppe horse according to Barker (1981), migrated between the uplands where they grazed on summer pastures and coastal lowlands where they overwintered. If these species didn't migrate then the hunter-gatherers would not find it necessary to move between coast and uplands. Using primarily oxygen stable isotope measurements along the growth direction of tooth enamel, they conclude that there was not consistent patterning of migratory behaviour as predicted by Higgs or Barker. This led to the favouring of Stiner's (Stiner et al., 2000) model of regional specialisation beginning during the Last Glacial Maximum. Yet, the inadequate chronological control available to studies such as Pellegrini et al. (2008) means that we cannot fully understand if variability in animal behaviour is strongly influenced by abrupt Late Quaternary climate change.

Grotta del Romito (southern Italy) preserves one of the most detailed sedimentary records of human occupation of the entire Italian Peninsula during the late last glacial period (e.g. Martini, 2002; Ghinassi et al., 2009; Craig et al., 2010; Martini and Lo Vetro, 2007; López-García et al., 2014). The cave was occupied almost uninterruptedly from the Last Glacial Maximum (LGM) to the Holocene, providing well-established cultural evidence related to Gravettian, Epigravettian, and more recently to Early Mesolithic and Neolithic cultures (Martini et al., 2007, 2016; Lo Vetro and Martini, 2016). Extraordinarily, the cave also contains rare evidence of Palaeolithic rock art and multiple intact human burials, making Grotta del Romito one of the most significant Upper Palaeolithic sites in the southern Europe.

In this study we have revised the Upper Palaeolithic chronostratigraphic framework of Grotta del Romito by applying Bayesian *Sequence* modelling (Bronk Ramsey, 2008) on new (Table 1) and existing radiocarbon dates performed on faunal, human and charcoals remains from the Gravettian to the Epigravettian levels. We have integrated the available depositional information (well-resolved sedimentary and cultural data), including the study of a tephra deposit with a great potential to become a regional marker for the onset of the last glacial interstadial, to generate a formal Bayesian model using the IntCal 13 calibration curve (Reimer et al., 2013). Built on the revised chronology, we compare the regional and North Atlantic palaeoclimate records (Brauer et al., 2007; Rasmussen et al., 2014) with available palaeoenvironmental information from the sedimentary deposits derived from micro and large mammals (Bertini Vacca, 2012; Bertini Vacca et al., 2012; López-García et al., 2014), and stable isotope analysis on land snail shells (Colonese et al., 2007). The results place the Last Glacial human occupation sequence of Grotta del Romito in a broad palaoenvironmental context and provide new chronological elements for understanding the cultural and environmental history of southern European refugia during the last Ice Age. This provides one of the most detailed site chronologies to date for an archaeological site covering this time period in Southern Europe. This, in turn, enables firmer assessment of human subsistence responses to abrupt climate changes at mid-latitude locations and even perhaps second order demographic responses, such as those suggested by important broader regional scale studies (e.g. Gamble et al., 2004, 2005).

2. Stratigraphic, archaeological and chronological settings

2.1. Palaeoclimatic setting

Climate conditions during the period of human occupation of the cave include cold periods such as the Last Glacial Maximum (LGM), which dates to ~26.5 to 19 ky BP (thousands of years Before Present) (Hughes et al., 2013), and the Heinrich 1 stadial, dated to ~ 17-16 ky BP (Rasmussen et al., 2014). There are additionally abrupt climatic shifts that characterise the transition from the Pleistocene to the Holocene, commonly known as the Last Glacial to Interglacial Transition (LGIT; Lowe et al., 2001). Key features of this period have been predominantly described in the North Atlantic realm and include abrupt warming and cooling events. The event stratigraphic scheme outlined by the INTegrating Ice core, MArine, and TErrestrial records (INTIMATE) group adopts the now commonly used term for these events as Greenland Interstadials (GI) for warm phases and Greenland Stadial (GS) events for cooling episodes. Moreover, the long GI-1 interstadial (~14,692–12,896 ice core years b2k; Rasmussen et al., 2014) is subdivided into five warm and cooler sub-stages. While initially defined for the North Atlantic region, climatic and environmental events observed in the Mediterranean region have been proposed as close correlatives of these North Atlantic events. For example, significant shifts in arboreal to non-arboreal pollen and vegetation biomes recorded in Mediterranean lacustrine sequences have been proposed as evidence of direct response of North Atlantic forcing (Allen et al., 1999; Tzedakis, 2005). Additional evidence for a coupled climate response between the Mediterranean and the North Atlantic comes from marine sea surface temperature records (Rohling et al., 2002; Siani et al., 2001, 2013). Finally isotopic variability in both marine and terrestrial palaeoenvironmental records from the Mediterranean have been, in part, attributed to North Atlantic climate forcing (e.g. Bar-Matthews et al., 1999; Robinson et al., 2006), although the interpretation of both carbon and oxygen isotopic variability in Mediterranean contexts is complicated by the competing influences of temperature and aridity (e.g. Candy et al., 2012). Nevertheless, there is substantial evidence for significant climate variability in the Mediterranean that is of importance for understanding *inter alia* the exact relationship between North Atlantic and Mediterranean climates; human adaptation to abrupt climate

Table 1
Romito radiocarbon ages and Bayesian age model maximum and minimum 95% HPDF ranges derived from the model shown in Table 2. Date codes in Bold are new ages from this study all other ages have been previously published (Martini et al., 2007; Craig et al., 2010; Martini and Lo Vetro, 2007; López-García et al., 2014). For ages generated for this study (shown in bold) we report $\delta^{13}C$ values and C/N ratio's along with the archaeological horizons that each date is derived from. For previously published data we also report the archaeological horizon and where available the $\delta^{13}C$ values.

Sample Code	14C age	error	$d^{13}C$	C/N	95% HPDF Max BP	95% HPDF Min BP	Layer
R_Date ROM 2	10,115	45	−20.85	3.2	12,073	10,948	B
R_Date ROM 1	11,000	45	−20.68	3.3	12,988	12,668	B
R_Date ROM 1a	11,035	45	−20.73	3.3	12,969	12,718	B
R_Date Beta-160,295	11,060	100	–		13,041	12,857	C
R_Date Beta-160,296	11,090	70	–		13,062	12,912	C2
R_Date ROM 3-1	11,075	50	−20.32	3.2	13,229	12,983	C3
R_Date ROM 3-2	11,060	40	−20.44	3.2	13,089	12,942	C3
R_Date Beta-160,297	11,380	70	–		13,182	12,933	C3
R_Date Beta-160,298	11,250	70	–		13,423	13,013	C4
R_Date ROM 4	14,305	65	−19.7	3.3	13,280	13,045	C4
R_Date Beta-160,299	11,580	70	–		13,489	13,278	D
R_Date Beta-160,300	11,660	70	–		13,670	13,361	D1
R_Date ROM 5-1	11,765	50	−20.53	3.4	13,831	13,328	D1
R_Date ROM 5-2b	12,415	50	−20.40	3.4	13,831	13,328	D1
R_Date Beta-160,302	12,060	90	–		14,064	13,794	D5a
R_Date Beta-160,303	12,160	50	−26		14,119	13,880	D5b
R_Date LTL234A	12,170	60	−26.8		14,165	13,939	D8
R_Date LTL238A	12,334	75	−24.7		14,406	14,080	D11
R_Date LTL607A	12,258	75	−24.4		14,561	14,144	D13
R_Date LTL603A	12,377	95	−30		14,630	14,215	D14
R_Date LTL608A	12,331	55	−25.3		14,696	14,275	D15
R_Date LTL601A	12,369	100	−28.3		14,797	14,335	D16
R_Date LTL602A	12,438	85	−26.9		14,943	14,450	D20
R_Date ROM 6-1	12,650	50	−20.40	3.5	15,113	14,740	D23
R_Date ROM 6-2	12,545	50	−19.67	3.5	15,070	14,684	D23
R_Date LTL1050A	12,494	75	−25.3		15,218	14,830	D29
Tephra					15,792	15,318	D30
R_Date LTL14264A	13,300	100	−26.9		16,008	15,138	D33
R_Date LTL1052A	12,970	150	–		16,173	15,210	D35
R_Date LTL1046A	13,650	120	−27.8		16,749	15,943	E2
R_Date ROM 7	15,230	70	−19.6	3.3	17,823	16,803	E5
R_Date LTL1047A	13,646	120	−32.8		17,029	16,194	E5
R_Date LTL1590A	14,373	90	−28.2		17,917	17,213	E8
R_Date LTL1591A	15,273	150	−33.6		19,103	18,033	E10
R_Date LTL1592A	16,129	100	−19.4		19,848	18,943	E16
R_Date LTL1593A	17,376	90	−21.6		21,365	20,638	F1
R_Date LTL239A	18,978	130	−30.8		22,978	21,918	F2
R_Date LTL606A	18,483	95	−26.5		22,997	22,212	F3I
R_Date LTL236A	19,351	180	−26.2		23,540	22,910	G1
R_Date LTL237A	19,373	90	−26		23,609	23,058	G2
R_Date LTL604A	20,210	245	−26		25,488	23,713	H4
R_Date LTL1048A	23,475	190	−23.5		28,003	26,958	I

change; and faunal responses to vegetation turnover. Due to the inherent influences of local and regional factors it is imperative to compare local evidence for changes with key regional palaeoclimate signals as well as important Northern Hemisphere stratotypes, such as the Greenland ice core records. Importantly for understanding the relationship between climate and patterns of human subsistence and dispersal it is necessary to be able to test the relationship between local and regional environments, where populations actually lived, and regional to global scale archives of climatic change, such as the Greenland ice cores that provide the overall climatic template.

2.2. Stratigraphic and archaeological record

Grotta del Romito is located in Calabria (39.054′ N 15.055′ E; Fig. 1), in southern Italy, and about 25 km inland from the Tyrrhenian Sea (Martini et al., 2003). The cave is set in Jurassic limestone underlain by Triassic dolomite and consists of a partially collapsed outer rockshelter and a main inner cave, which were connected during the Palaeolithic period to form a large cavity (Figs. 1–4). The site was first excavated in the 1960s by Paolo Graziosi (Graziosi, 1962, 1971), who opened archaeological trenches both in the cave and under the rock-shelter (Fabbri et al., 1989). From 2000 onwards new archaeological excavations expanded the former trench within the cave bringing to light well-preserved Palaeolithic and Mesolithic deposits (Martini and Lo Vetro, 2005a,b, 2007, 2011; Martini et al., 2007, 2016).

The inner stratigraphic sequence subject to the present study is composed of twelve main archaeological units (Layers A – N), containing archaeological levels (often recognisable as palaeosurfaces) covering a period from ~23 to 10 ky uncal. BP (Martini et al., 2007; Ghinassi et al., 2009; Martini and Lo Vetro, 2011). These units include material culture associated to the Middle-Late Gravettian (units N, M, L, I, H, G), Early Epigravettian (F), and Evolved to Late Epigravettian (E, D) (Figs. 2 and 3). The main subdivisions of the stratigraphic units (or layers) are based on changes in lithology, while archaeological levels are used to define sub units (or sub-layers). The layers are predominantly coarse-to fine-grained cave sediments, derived from weathered limestone and inwashed sediment, with additional larger clasts of deposited limestone, although there is a significant shift between units E and D, with the former consisting predominantly of a mix of alluvially derived sediments and the latter comprising mainly anthropogenic sediments (Ghinassi et al., 2009), reflecting increased human

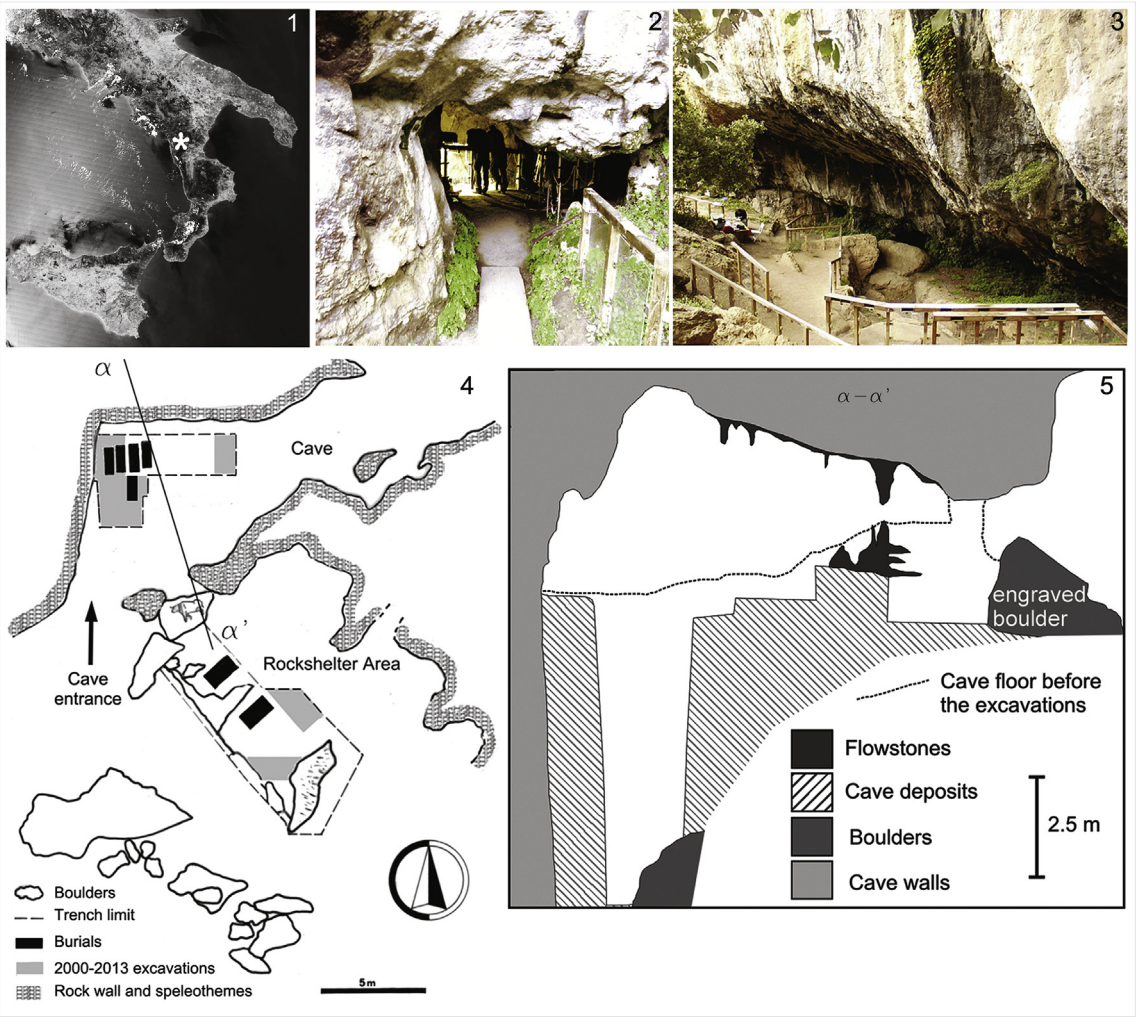

Fig. 1. Location map of Grotta del Romito (1) and the cave entrance (2–3). The Rock shelter, general view from est. Plan of the site showing the distribution of the archaeological trenches and burials (4). Cross-section of the site and of the excavated area along the axis a-a' indicated in the plan (5) (nos. 2–4 modified after Martini and Lo Vetro, 2011).

occupation from unit D onwards at the deactivation of the water runoff inside the cave.

The sedimentary deposit within the cave is generally well-ordered, although few disturbances occurred due to a series of human burials and other archaeological features (e.g. pits), especially in the upper part of the sequence (units D and C). Deposits A and B were heavily disturbed by Neolithic and historical activities, and A is not considered in this paper, although we have tested samples from B. A useful stratigraphic marker within the cave stratigraphy is the presence of a visible tephra layer within unit D30. This layer has not until now been chemically analysed or associated to any known Italian volcanic deposits and, thus, analysis of this deposit is an additional objective of the chronological re-evaluation of this sedimentary record.

The outer rockshelter preserves sediments dated to the Early Holocene (Early Mesolithic and Middle Neolithic) superimposing a Terminal Pleistocene (Late Epigravettian) deposit that partially matches to the upper part of the inner sequence.

The archaeological relevance of Grotta del Romito lies notably on the presence of rock art and nine intact Upper Palaeolithic human burials (ROMITO 1-9) dated to the Epigravettian; (Graziosi, 1962, 1971; Fabbri et al., 1989; Martini, 2006; Craig et al., 2010; Martini and Lo Vetro, 2007; De Silva et al., 2016), a detailed archaeological record of increasing intensification of human occupation and abundant Late Pleistocene micro and large mammal remains (Fig. 2) representing distinct environments and subsistence strategies over thousands of years (Martini et al., 2007; Bertini Vacca, 2012; Bertini Vacca et al., 2012; López-García et al., 2014). Snail shells were also recovered from the archaeological deposit. Their stable isotope and taxonomic composition reveals considerable environmental changes during the later phase of occupation of the site (Colonese et al., 2007).

2.3. Radiocarbon dates

The radiocarbon data for Grotta del Romito span from the LGM to the end of the LGIT and are reported in Table 1 in relation to the archaeological units and sub-units. The site chronology is underpinned by 24 stratigraphically consistent radiocarbon ages performed on charcoal (Martini et al., 2007; Craig et al., 2010; Martini and Lo Vetro, 2007; López-García et al., 2014). Most of these samples were analysed at CEDAD radiocarbon facilities (Lecce), and a few at Beta Analytic (Miami). Samples from the Lecce radiocarbon laboratory are also reported with $\delta^{13}C$ values, which are used as both a correction for sample fractionation but also as a guide to some forms of sample contamination. For example, in chalk and limestone dominated geology less negative $\delta^{13}C$ values, closer to those normally associated with marine carbonates, may indicate

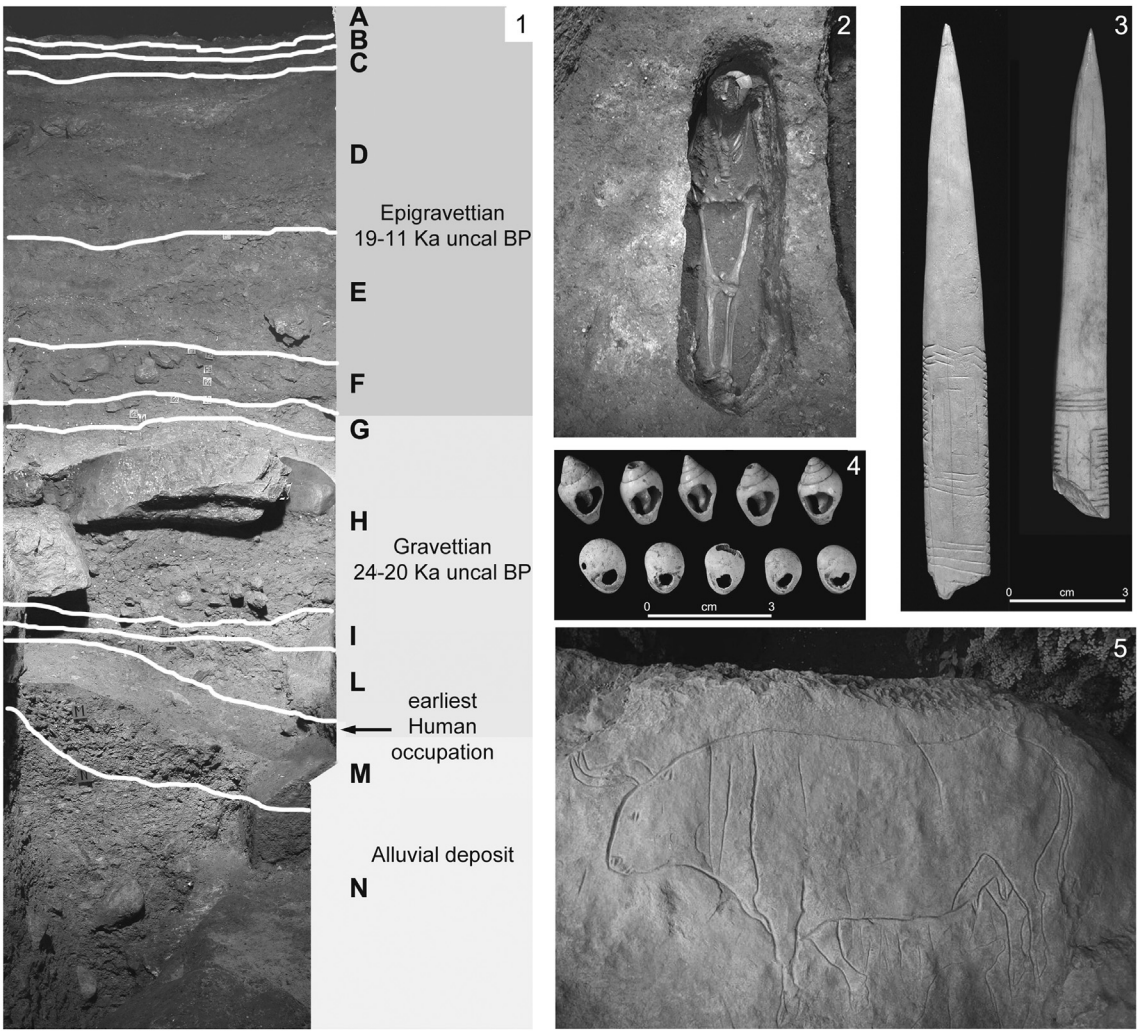

Fig. 2. The general stratigraphic sequence (layers A-N), picture of the section east of the trench excavated inside the cave; 1. Some of the Final Epigravettian evidence: the burial Romito 8 (2), engraved bone points (3), ornamental marine molluscs shells (4), rock art (*Bos primigenius*) in the rock-shelter located right to the cave entrance (5) (modified after Martini and Lo Vetro, 2011).

the potential from some geological (dead) carbon contamination of the sample, and the potential for dates to be too old. In the case of the Grotta del Romito samples $\delta^{13}C$ values are predominantly in the range expected for terrestrial C3 organic material and while there is some scatter in the range charcoal values are normally in the range of −25‰ and faunal material in the range of ~ −20‰. These data are supplemented by three AMS radiocarbon determinations on human burials from the site (Craig et al., 2010). Of these, one sample (LTL3033A) comes from the rock shelter levels lying outside the main Grotta del Romito sequence and does not form part of this age modelling exercise. However, it does provide a constraining age for the sequence within the cave. The direct date for ROMITO 9, sample LTL3034A (layer E16), a burial disturbed *ab antiquo* (Martini and Lo Vetro, 2011), is inconsistent with the AMS data of Layer E16 and also with the chronological sequence of the layer E. The direct date for ROMITO 3, sample LTL3032A, from a burial excavated in the 1960's, is also problematic as there is some degree of uncertainty in the exact stratigraphic position of this burial, although it is quite consistent with the chronology of the other Late Epigravettian burials unearthed inside the cave. Both Romito 9 and Romito 3 direct data are thus excluded from further consideration.

In addition to these data here we present new AMS radiocarbon determinations from animal tooth samples (ROM-1 to ROM-7; Table 1). These dates all have securely recorded association to a particular stratigraphic layer within the cave sequence, and were all initially considered as part of the age modelling process. Tooth samples were selected for analyses for a number of reasons. Firstly, the dentine from these samples were highly suitable for extraction and preparation of collagen by ultrafiltration (e.g. Rodríguez-Rey et al., 2015); secondly, analyses of strontium and oxygen isotopes from the tooth samples (Pellegrini et al., in preparation) will allow further understanding of faunal mobility within the site and surrounding region. Additionally, while the archaeological assignment to a particular stratigraphic layer is secure, due to the potential for material to be moved due to human deposit-reworking, and the general quality assurance issues in archaeological radiocarbon dating (e.g. Housley et al., 1997; Pettitt et al., 2003; Blockley et al., 2006; Higham et al., 2006, 2009), a result of this age modelling process is an evaluation of how well the new tooth AMS dates fit in with their assigned position in the units and sub-units of the Grotta del Romito sequence and the overall site chronology.

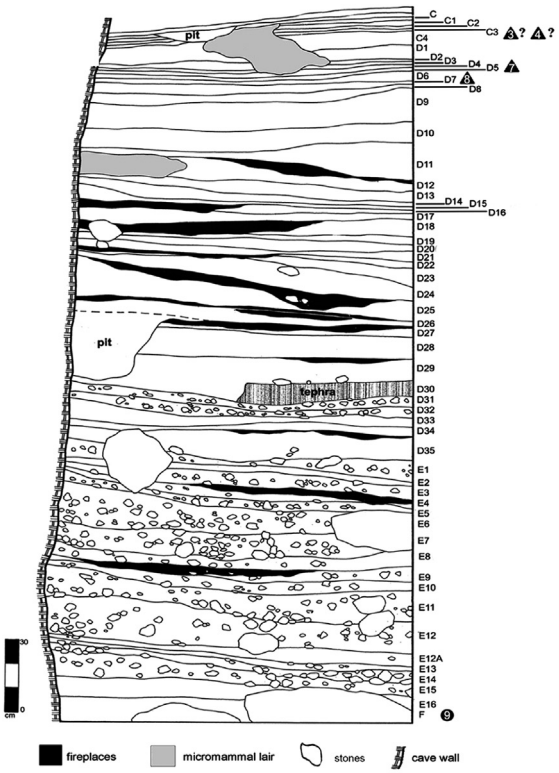

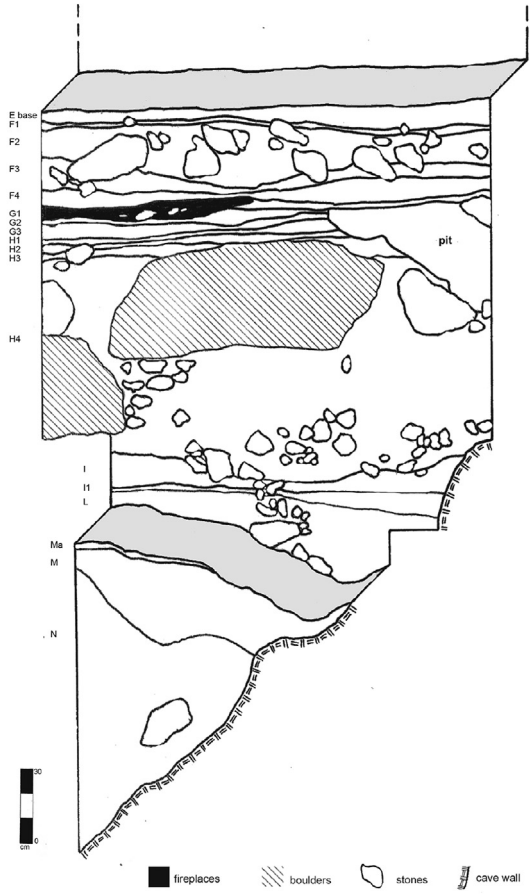

2.4. Tephra

The Grotta del Romito record also contains a visible tephra layer within unit D 30 of the stratigraphic sequence, which is a rare occurrence in late Pleistocene archaeological records from this region of Italy. Given this, along with the fact that Grotta del Romito is an important Late Upper Palaeolithic record for the region, it is an important objective of this study to chemically classify this tephra and calculate its likely age for future studies, and if possible correlate it to known volcanic eruptive records.

3. Methods

3.1. Age modelling

The predominantly well-ordered stratigraphic deposit of the Grotta del Romito (Fig. 3), and the fact that the majority of the radiocarbon ages were sampled from hearth units within defined cultural layers (Table 1), make this sedimentary record suitable for Bayesian sequence analyses. The radiocarbon ages from the site reveal a sequentially ordered age depth relationship. In order to assess the age versus depth relationships a Bayesian modelling approach was adopted. There are a number of potential models available for a depositional sequence within the programme OxCal, with different Bayesian *Priors* that are deemed to be appropriate for differing levels of prior information about a sequence. These range from a *Phase* model, comprising an unordered group or set of groups (Bronk Ramsey, 2009a), through *Sequence* models, for ordered groups, that utilise the principles of stratigraphy and succession as part of the prior model. More recently these have been further developed into models that incorporate sediment deposition through a Poisson model of sediment formation (*P_Sequence*; Bronk Ramsey, 2008; 2009a; Blockley et al., 2008).

While all of these models have been applied successfully in Quaternary records, a *Sequence* model with nested *Phases* is deemed most appropriate for Grotta del Romito and is applied in this study. The stratigraphy of the site comprises an ordered sequence of layers and sub-layers, with radiocarbon dates on archaeological horizons, hence a sequential model is suitable. In some of the sub-layers, however, there are several ages with no internal stratigraphic order, as they are sampled from different structures (i.e. hearths) or areas in the same sub-layer. In these cases only their assignment to a stratigraphic sub-unit and its overall position within the scheme is available. Multiple dates on the same stratigraphic layer in different parts of the site are included in the model as nested phases within the overall sequence (e.g., Buck et al., 1991 for the principle of sequences and nested phases). Such models have been used in numerous archaeological sites and have been particularly effective in long cave records such as Grotta del Romito (e.g. Clark-Balzan et al., 2012).

The *Sequence* model is *a priori*; it incorporates the laws of stratigraphy and succession and assumes that age should increase with depth, along with the radiocarbon dates and calibration information (i.e. IntCal13; Reimer et al., 2013). In addition, in order to recognise the potential for unconformities or differences in deposition between the main lithological boundaries (B-G) these units are separated by *Boundaries*. These are functions used within many

Fig. 3. Epigravettian stratigraphic sequence (layers A-F) drawn from the section north of the trench excavated inside the cave; the Triangles and the circle indicate the position of the burials. Triangles with question mark (?) shows the probable stratigraphic position of Romito 3 and Romito 4 burials found by Graziosi in 1964 (Romito stratigraphy modified after Martini and Lo Vetro, 2011). The age model is broken down into individual segments in the supplementary information section to allow a more detailed view.

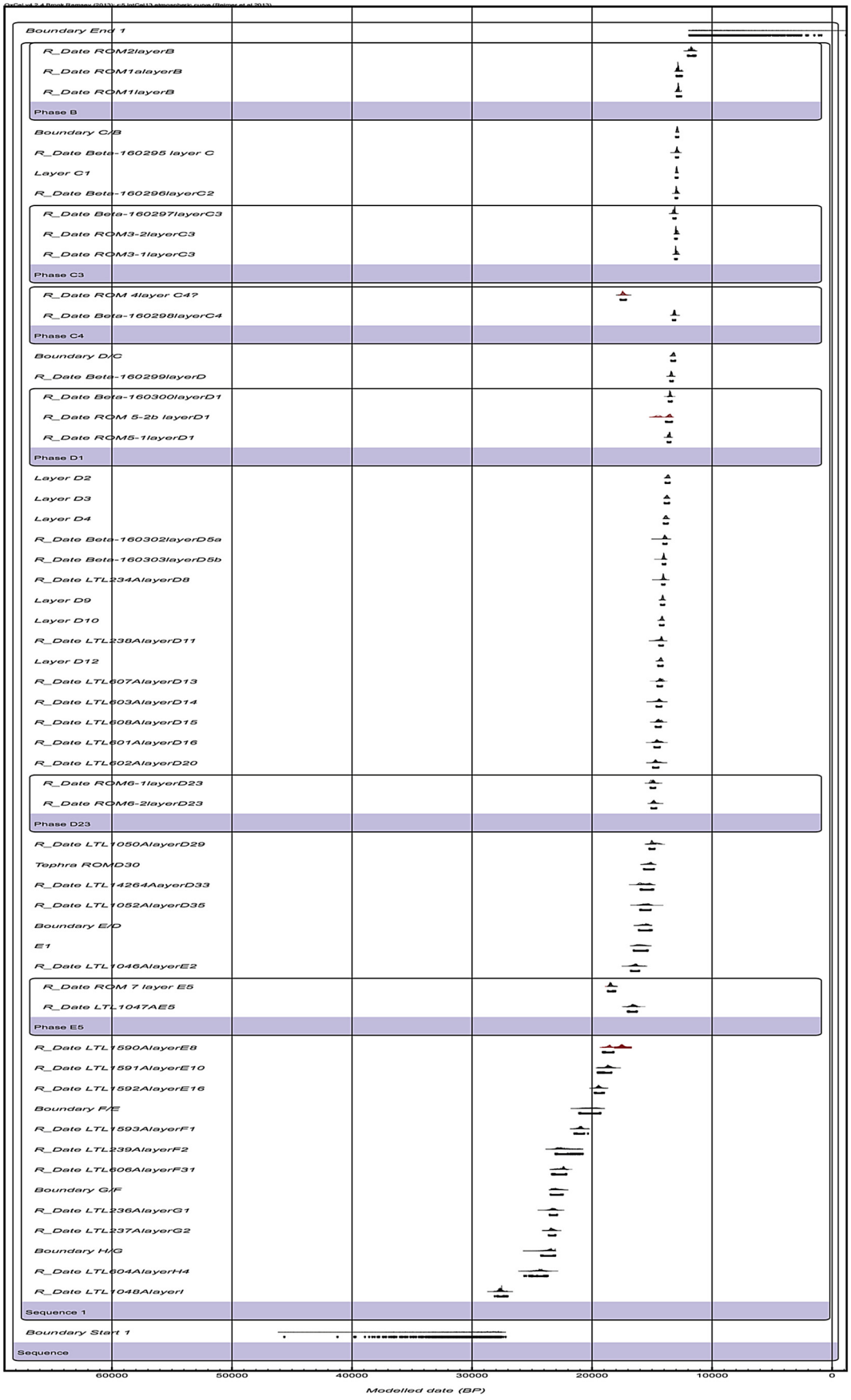

Fig. 4. Bayesian age model output for Romito showing the entire record (4a) also showing HPDF's for sub units with no measured radiocarbon age, calculated from their position within the sequence in relation to the dated sub-layers and the model prior. The three dates identified as fully outlying by the outlier model are coloured in red. A detailed breakdown of this model is shown in supplementary information. (For interpretation of the references to colour in this figure legend, the reader is referred to the web version of this article.)

Bayesian age modelling priors that allow the separation of different units within a model (see Bronk Ramsey, 2008). Each calibrated radiocarbon date is constrained during the calibration process by the stratigraphic succession, the calibration curve and the ranges of all the other dates in the sequence, to produce a Highest Probability Density Function (HPDF) for each date (Fig. 4, Tables 1–3) in the model and their assignment to individual sub-layers within the strata. While most of the sub-units in the cave contain material suitable for radiocarbon dating, at least in the time period under study, some sub-units do not have assigned ages. Within a *Sequence* model it is possible to infer the likely ranges for events between dated horizons, with varying degrees of uncertainty. Here a small number of undated layers between dated layers (sub units C1, D2-4, D9 and D12) have had their ages estimated from their relative sequential position within the model. These have been incorporated as they contain evidence for human presence and are thus important for any discussion of the pattern of human occupation in relation to environmental change. We have not, however, attempted any further constraints on the chronology, by, for example, applying a depositional *P_Sequence* model. This is due to the nature of human occupation of the site potentially leading to disturbed layers. This means that while we would expect the site predominantly to respect our simple constraint that age should increase with stratigraphic depth we are less sure that we are recording continuous deposition, and thus have not attempted deposition modelling. Our primary model is, thus, ordered by stratigraphic position within the sequence and this is used in all of the main outputs from this exercise (Table 2 and Figs. 4, 7–9, with outlier information in Table 3). We have, however, also run a second variant of the model (Table 4a) where we have retained the straitgraphic ordering but also grouped dates in to separate sequences by their archaeological cultural affinities (Evolved Gravettian [units M-L-I]; Late Gravettian [units H-G]; Early Epigravettian [unit F]; Evolved Epigravettian [unit E]; Late Epigravettian [units D,C,B]). This separation allows us to calculate the timing of the transitions between the cultural layers and the spans of each of the phases of occupation of the site. This also shows (Table 4b) the composition of the sedimentary facies and sedimentary units of each of the different cultural zones.

It is also essential, in this case, to address the potential for individual dates to be outliers. There has been much debate as to the best approach to dealing with outliers in Bayesian modelling. Approaches include using the level of agreement between Prior age distributions and Posterior model output as a criteria for questioning dates (Blockley et al., 2004). More recently Bayesian formal approaches proportionally reduce the influence of likely outlying dates (Bronk Ramsey, 2009b) and the overall likelihood of any given date being an outlier can be set *a priori*. Here we adopt the formal automatic outlier detection approach outlined in Bronk Ramsey (2009b) and have applied the General (t) Outlier model, because likely causes for outliers include issues of radiocarbon pretreatment but also stratigraphic reworking (cultural and bioturbation). As the sequence stratigraphy is relatively well defined we have set the possibility for any individual date to be an outlier at 5% and outliers are reported in Table 3 and discussed in the text in more detail.

3.2. Tephrochronology

Importantly the main cave sequence has a visible tephra horizon in layer D30 (ROM-D30 hereafter), at a mid-point depth, relative to the cave datum, of 220 cm below datum and with an average thickness of 10 cm. This is underlying to a layer that has yielded a radiocarbon sample with an age of 12,494 ± 75 b.p. placing this tephra around the period of the transition between the GS-2 stadial and the onset of GI-1 in the INTIMATE event stratigraphy (Rasmussen et al., 2014). While the final model age for this tephra will be discussed below it is worth noting that the radiocarbon age suggests that it is slightly older than the widespread Neapolitan Yellow Tuff (NYT) eruption that occurs in the early part of GI-1 with a reported radiocarbon age of 12,100 ± 170 b.p (Siani et al., 2004). In order to better constrain the provenance of the Romito-D30 tephra, samples were taken for WDS-EPMA (Wavelength Dispersive Electron Probe Micro Analyses) at the University of Oxford. Glass from top, middle and base of the visible tephra unit (samples RH295, 296, 297, 298, 299 and 301) were sieved through 125 μm and 15 μm mesh sizes and mounted onto stubs and coated in resin. They were then ground and polished to a 0.25 μm before carbon coating. Samples were run using the protocols outlined for the RESET project (e.g. Lowe et al., 2012), with a beam diameter of 10 μm and a current of 5 nA. This generated major and minor element data (Table 2) for 9 oxides and these were compared to a large geochemical data set from the RESET project and from the published literature including proximal tephra units, long lacustrine archives and Adriatic marine cores (Wulf et al., 2004, 2008; Siani et al., 2004; Tomlinson et al., 2012; Matthews et al., 2015). Glass reference standards were run routinely during the analyses to check for instrumental drift and are available as supplementary data. The majority of the data used for comparison comes from the RESET project (Tomlinson et al., 2012) and the samples analysed in both this study and the RESET project use the same EPMA facility and the same operating conditions. For data derived from projects outside RESET (Wulf et al., 2004, 2008) instrument operating conditions were comparable to those used in this study. While Wulf et al. (2004, 2008) studies differ in terms of secondary standards, a number of comparative analyses have been successfully undertaken between that data set and more recently generated data using the RESET protocols (e.g. Lane et al., 2011; Albert et al., 2013). We are thus confident that these data are able to underpin the attempted correlation of the ROM-D30 tephra.

4. Results

4.1. Age modelling and outlier assessment

The results of the *Sequence* age model are presented in Fig. 4a–e showing the model broken down into sections and presented numerically in Tables 1 and 2, with the results of outlier detection reported in Table 3 and the adapted model to calculate span functions in Table 4. While most ages conformed well to the model prior with HPDF posterior distributions matching well, in some cases some prior ages for tooth samples are significantly different to the posterior distributions. This is confirmed by outlier reports (supplementary information) that show ROM4 and ROM5-2b to be 100% outside of the range that would be consistent with the model and thus have not provided any input into the model (e.g. Bronk Ramsey, 2009b). These two tooth samples are likely to have been moved in the sequence due to human activity, both having prior ages much more consistent with older layers (sub unit E5 for ROM D4 and sub unit D14 for ROM5-2b). In addition, tooth sample ROM7 was also highlighted as an outlier with 72% of the age distribution falling outside the range consistent with the model and the other dates. In this case due to the bimodal distribution of the calibrated date due to shape of the calibration curve at this point, this age could be consistent with layers from E8 through to E10. Finally tooth sample ROM2, taken from the same layer as ROM1 and

Table 2
Oxcal model output for the Romito stratigraphic sequence showing the ordering of the dates, nested phases where needed and the modelled ages of undated layers based on their relative positions in the sequence compared to dated units.

Name	Unmodelled (BP)			Modelled (BP)		
	from	to	%	from	to	%
Boundary End 1				12,013	−5142	95.6
R_Date ROM2layerB	11,998	11,407	95.3	12,073	10,948	95.4
R_Date ROM1alayerB	13,039	12,763	95.4	12,988	12,668	95.4
R_Date ROM1layerB	12,997	12,735	95.4	12,969	12,718	95.3
Phase B						
Boundary C/B				13,039	12,829	95.4
R_Date Beta-160,295 layer C	13,088	12,731	95.4	13,041	12,857	95.4
Layer C1				13,050	12,880	95.4
R_Date Beta-160296layerC2	13,090	12,783	95.4	13,062	12,912	95.4
R_Date Beta-160297layerC3	13,367	13,083	95.4	13,229	12,983	95.4
R_Date ROM3-2layerC3	13,050	12,800	95.4	13,089	12,942	95.4
R_Date ROM3-1layerC3	13,068	12,801	95.4	13,182	12,933	95.4
Phase C3						
R_Date ROM 4layer C4	17,631	17,185	95.4	13,423	13,013	95.4
R_Date Beta-160298layerC4	13,273	12,996	95.4	13,280	13,045	95.4
Phase C4						
Boundary D/C				13,431	13,018	95.3
R_Date Beta-160299layerD	13,554	13,283	95.4	13,489	13,278	95.4
R_Date Beta-160300layerD1	13,704	13,313	95.4	13,670	13,361	95.4
R_Date ROM 5-2b layerD1	14,861	14,175	95.4	13,831	13,328	95.5
R_Date ROM5-1layerD1	13,728	13,469	95.4	13,712	13,466	95.4
Phase D1						
Layer D2				13,897	13,531	95.4
Layer D3				13,966	13,584	95.4
Layer D4				14,038	13,668	95.4
R_Date Beta-160302layerD5a	14,150	13,730	95.4	14,064	13,794	95.4
R_Date Beta-160303layerD5b	14,188	13,842	95.4	14,119	13,880	95.4
R_Date LTL234AlayerD8	14,226	13,826	95.4	14,165	13,939	95.4
Layer D9				14,262	13,982	95.4
Layer D10				14,348	14,029	95.4
R_Date LTL238AlayerD11	14,775	14,059	95.4	14,406	14,080	95.4
Layer D12				14,456	14,109	95.4
R_Date LTL607AlayerD13	14,646	13,960	95.4	14,561	14,144	95.5
R_Date LTL603AlayerD14	14,952	14,087	95.4	14,630	14,215	95.4
R_Date LTL608AlayerD15	14,687	14,087	95.4	14,696	14,275	95.5
R_Date LTL601AlayerD16	14,958	14,072	95.4	14,797	14,335	95.4
R_Date LTL602AlayerD20	15,016	14,170	95.4	14,943	14,450	95.4
R_Date ROM6-1layerD23	15,232	14,778	95.4	15,113	14,740	95.4
R_Date ROM6-2layerD23	15,126	14,473	95.4	15,070	14,684	95.4
Phase D23						
R_Date LTL1050AlayerD29	15,083	14,263	95.4	15,218	14,830	95.4
Tephra ROMD30				15,817	14,933	95.5
R_Date LTL14264AayerD33	16,280	15,701	95.4	16,008	15,138	95.5
R_Date LTL1052AlayerD35	15,989	15,109	95.4	16,173	15,210	95.5
Boundary E/D				16,317	15,233	95.5
R_Date LTL1046AlayerE2	16,900	16,128	95.4	16,749	15,943	95.4
R_Date ROM 7 layer E5	18,680	18,320	95.4	17,823	16,803	95.4
R_Date LTL1047AE5	16,894	16,120	95.4	17,029	16,194	95.3
Phase E5						
R_Date LTL1590AlayerE8	17,808	17,218	95.4	17,917	17,213	95.4
R_Date LTL1591AlayerE10	18,843	18,169	95.4	19,103	18,033	95.4
R_Date LTL1592AlayerE16	19,756	19,167	95.4	19,848	18,943	95.3
Boundary F/E				21,040	19,163	95.4
R_Date LTL1593AlayerF1	21,275	20,685	95.4	21,365	20,638	95.4
R_Date LTL239AlayerF2	23,230	22,495	95.4	22,978	21,918	95.4
R_Date LTL606AlayerF31	22,562	22,052	95.4	22,997	22,212	95.4
Boundary G/F				23,498	22,403	95.4
R_Date LTL236AlayerG1	23,791	22,858	95.4	23,540	22,910	95.4
R_Date LTL237AlayerG2	23,607	23,025	95.4	23,609	23,058	95.3
Boundary H/G				24,295	23,116	95.5
R_Date LTL604AlayerH4	25,065	23,735	95.4	25,488	23,713	95.4
R_Date LTL1048AlayerI	27,926	27,357	95.4	28,003	26,958	95.3
Sequence 1						
Boundary Start 1				46,083	27,473	96.7
Sequence						
U(0,4)	3.99E-17	4	95.4	2.28	2.52	95.4
T(5)	−2.65	2.65	95.4			
Outlier_Model General				−4567	853	95.6

Table 3
Reported outlier values for the Romito radiocarbon ages using the General outlier model (Bronk Ramsey, 2009b) and a 5% probability of any date being outlying. LTL606, LTL239, LTL1590, LTL14264, ROM 5-2 and ROM 4 are all significant outliers, however, the majority of the dates conformed well to stratigraphic ordering.

Element	Prior	Posterior	Model	Type
LTL1048AlayerI	5	4	General	t
LTL604AlayerH4	5	4	General	t
LTL237AlayerG2	5	2	General	t
LTL236AlayerG1	5	2	General	t
LTL606AlayerF31	5	37	General	t
LTL239AlayerF2	5	50	General	t
LTL1593AlayerF1	5	4	General	t
LTL1592AlayerE16	5	3	General	t
LTL1591AlayerE10	5	13	General	t
LTL1590AlayerE8	5	100	General	t
LTL1047AE5	5	3	General	t
ROM 7 layer E5	5	7	General	t
LTL1046AlayerE2	5	3	General	t
LTL1052AlayerD35	5	3	General	t
LTL14264AayerD33	5	62	General	t
LTL1050AlayerD29	5	8	General	t
ROM6-2layerD23	5	2	General	t
ROM6-1layerD23	5	4	General	t
LTL602AlayerD20	5	2	General	t
LTL601AlayerD16	5	2	General	t
LTL608AlayerD15	5	2	General	t
LTL603AlayerD14	5	2	General	t
LTL607AlayerD13	5	3	General	t
LTL238AlayerD11	5	2	General	t
LTL234AlayerD8	5	1	General	t
Beta-160303layerD5b	5	1	General	t
Beta-160302layerD5a	5	1	General	t
ROM5-1layerD1	5	1	General	t
ROM 5-2b layerD1	5	100	General	t
Beta-160300layerD1	5	1	General	t
Beta-160299layerD	5	1	General	t
ROM 4 Layer C4	5	100	General	t
Beta-160298layerC4	5	2	General	t
ROM3-1layerC3	5	3	General	t
ROM3-2layerC3	5	4	General	t
Beta-160297layerC3	5	5	General	t
Beta-160296layerC2	5	1	General	t
Beta-160,295 layer C	5	1	General	t
ROM1layerB	5	2	General	t
ROM1alayerB	5	9	General	t
ROM2layerB	5	3	General	t

ROM1a (layer B) has an 82% chance of outlying the distribution of the model, and in this case is younger than the range for other dates in this layer and could have been worked down from the upper disturbed layer A. Thus, of the 11 tooth samples from this study 4 appear out of position in the sequence. This is not surprising given the potential for sediment reworking in cultural deposits in Mediterranean caves (Woodward and Goldberg, 2001), however the potential for good collagen preservation in these samples, plus the fact they provide potential for useful future tooth enamel isotope studies, demonstrates their overall usefulness.

Beyond the tooth ages, outlier analyses were performed on all of the dates used in the age model as part of the *Sequence* model. These ages showed a high degree of conformity to the model prior, again not surprising given the simple uniform prior and the assumption of sequential deposition. Only LTL239A showed a high likelihood of being an outlier (63%) reflecting the fact that the samples are taken from defined archaeological units within the sedimentary sequence and that for a simple prior that the rules of stratigraphy and succession should apply. The age model now forms the basis for further chronological, archaeological and environmental analyses for the site within its wider regional context.

The results of the second model, where as well as stratigraphic ordering the dates were also separated by cultural attribution are shown in Table 4. The details of this are discussed in section 5.

4.2. Tephrochronolgy

EPMA analyses of the ROM-D30 visible tephra (Table 5) indicate a compositionally heterogeneous layer (SiO_2 = 58.0–65.2 wt%; CaO = 1.5–4.7; $Na_2O + K_2O$ = 11.2–13.5 wt%; n = 136) with glasses ranging from phono-trachytic to trachytic in composition (Fig. 5). Within this heterogeneity, two main compositional populations can be observed; (1) a dominant high-K phono-trachytic component (~60.3 wt% SiO_2; ~9.3 wt% K_2O) where $K_2O \gg Na_2O$ (Na_2O = 3.5 wt%), and (2) a more evolved population with a high-K trachytic composition (~62.4 wt% SiO_2), slightly lower K_2O (~8.7 wt %) and higher Na_2O (~4.5 wt%) (Fig. 5).

5. Discussion

5.1. Correlation and stratigraphic importance of the ROM-D30 tephra

The results indicate that ROM-D30 must derive from older Pre-NYT activities associated with the Tufi Biancastri eruptive succession, which encompasses a series of eruptions between the Campanian Ignimbrite (CI) and the NYT (Orsi et al., 1996). The dominant high-K phono-trachytic glass population of ROM-D30 does not appear to correlate to any of the currently characterised proximal Campi Flegrei (CF) tephra units during this period, however, the glass compositions of many eruptive units within the Tufi Biancastri are yet to be thoroughly characterised. The other glass population of the ROM-D30 layer is consistent with the K-trachytic glasses that were repeatedly erupted at CF caldera during this post-CI and Pre-NYT period (e.g. eruptive units PRa, VRa, VRb; Fig. 6; data from Tomlinson et al., 2012, 2014; 2015). Thus, the glass compositional data presented here indicate that the D30 tephra layer clearly derives from explosive volcanism within the CF caldera, but based on the available proximal geochemical datasets it is not possible at this time to establish a precise proximal-distal tephra correlation within the Post-CI/Pre-NYT succession.

There are numerous tephra layers from CF caldera dispersed into distal areas during the period immediately prior to the NYT that are recognised in sedimentary archives. Fig. 6b compares the compositional data of ROM-D30 layer to CF derived tephra recorded in downwind archives such as Lago Grande di Monticchio (LGdM), and two Adriatic marine cores (MD90917 [Siani et al., 2004] and SA03-11 [Matthews et al., 2015]). At LGdM four K-trachytic layers (TM-10a, TM-10b, TM-10c and TM-10d) are recorded between 15,550 ± 780 and 15,030 ± 750 cal BP (Wulf et al., 2008). Based on glass data presented here we can tentatively suggest that LGdMTM-10a (15,030 ± 750 cal BP) may offer the most reliable distal-distal correlative of the D30 layer. The modelled age of the ROM-D30 tephra from Table 2 is 15,792–15,318 cal BP (IntCal 13) and this comfortably overlaps with the TM-10a age. However, the complexity of precisely correlating distal tephra layers in this time interval is illustrated by existing correlations associated with these TM-10 (a-d) layers. Wulf et al. (2008) correlate all four of these LGdM layers to the Lagno Amendolare (LAM) tephra unit, however, average glass compositions of the LAM are inconsistent with our ROM-D30 tephra, as best illustrated by their more elevated K_2O (Fig. 6a). Conversely, the average composition of the distal marine tephra layer MD90917 434 cm from the southern Adriatic, again correlated to the more proximal LAM tephra by Siani et al. (2004), appears to be broadly similar in composition to the dominant glass population of the D30 tephra (Fig. 6b). The absence of an unequivocal correlative for the ROM-D30 tephra in either in the proximal or distal setting means that, for now, this layer cannot

Table 4a
The outputs from the revised model set up as multiple stratigraphically ordered sequences arranged by cultural attribution to allow spans and transition times between different cultures to be calculated. Groups were organised as follows: Evolved Gravettian [units M-L-I, dates only available for unit I]; Late Gravettian [units H-G]; Early Epigravettian [unit F]; Evolved Epigravettian [unit E]; Late Epigravettian [units D,C,B]. The sediment types for each of the layers is also shown.

Name	Modelled (BP) 95%			
	from	to	%	Layer
Boundary End Late Epigravettian	**12,013**	**11,297**	95.4	
Span Late Epigravettian	**3543**	**4348**	95.4	
R_Date Â R_Date ROM 2	12,034	11,622	95.4	B
R_Date Â R_Date ROM 1	12,916	12,725	95.4	B
R_Date Â R_Date ROM 1a	12,930	12,731	95.4	B
Phase B				
R_Date Â R_Date Beta-160,295	12,985	12,805	95.4	C
R_Date Â R_Date Beta-160,296	13,018	12,844	95.4	C2
R_Date Â R_Date ROM 3-1	13,079	12,901	95.4	C3
R_Date Â R_Date ROM 3-2	13,070	12,895	95.4	C3
R_Date Â R_Date Beta-160,297	13,246	13,068	95.4	C3
Phase C3				
R_Date Â R_Date Beta-160,298	13,291	13,101	95.4	C4
R_Date Â R_Date Beta-160,299	13,496	13,274	95.4	D
R_Date Â R_Date Beta-160,300	13,710	13,376	95.4	D1
R_Date Â R_Date ROM 5-1	13,728	13,470	95.4	D1
Phase D1				
R_Date Â R_Date Beta-160,302	14,041	13,735	95.4	D5a
R_Date Â R_Date Beta-160,303	14,121	13,865	95.4	D5b
R_Date Â R_Date LTL234A	14,191	13,972	95.4	D8
R_Date Â R_Date LTL238A	14,317	14,052	95.4	D11
R_Date Â R_Date LTL607A	14,415	14,098	95.4	D13
R_Date Â R_Date LTL603A	14,534	14,154	95.4	D14
R_Date Â R_Date LTL608A	14,641	14,216	95.4	D15
R_Date Â R_Date LTL601A	14,770	14,292	95.4	D16
R_Date Â R_Date LTL602A	14,922	14,424	95.4	D20
R_Date Â R_Date ROM 6-1	15,106	14,744	95.4	D23
R_Date Â R_Date ROM 6-2	15,073	14,662	95.4	D23
Phase D23				
R_Date Â R_Date LTL1050A	15,180	14,848	95.4	D29
R_Date Â R_Date LTL14264A	15,984	15,363	95.4	D33
R_Date Â R_Date LTL1052A	16,090	15,456	95.4	D35
Sequence Late Epigravettian				
Boundary Transition Evolved/Late Epigravettian	**16,375**	**15,549**	95.4	
Span Evolved Epigravettian	**2631**	**3456**	95.4	
R_Date R_Date LTL1046A	16,700	16,101	95.4	E2
R_Date R_Date ROM 7	18,047	17,882	95.4	E5
R_Date R_Date LTL1047A	16,935	16,290	95.4	E5
Phase E5				
R_Date R_Date LTL1590A	18,085	17,895	95.4	E8
R_Date R_Date LTL1591A	18,841	18,176	95.4	E10
R_Date R_Date LTL1592A	19,733	19,152	95.4	E16
Sequence Evolved Epigravettian				
Boundary Transition Early/Evolved Epigravettian	**21,017**	**19,344**	95.4	
Span Early Epigravettian	**1221**	**1925**	95.4	
R_Date R_Date LTL1593A	21,292	20,696	95.4	F1
R_Date R_Date LTL239A	22,687	22,371	95.4	F2
R_Date R_Date LTL606A	22,760	22,402	95.4	F3I
Sequence Early Epigravettian				
Boundary Transition Late Gravettian/Early Epigravettian	**23,347**	**22,505**	95.4	
Span Late Gravettian	**265**	**1776**	95.4	
R_Date R_Date LTL236A	23,526	22,910	95.4	G1
R_Date R_Date LTL237A	23,653	23,131	95.4	G2
R_Date R_Date LTL604A	24,913	23,576	95.4	H4
Sequence Late Gravettian				
Boundary Transition Evolved/Late Gravettian	**27,592**	**23,733**	95.4	
Span Evolved Gravettian	**0**	**5**	95.4	
R_Date R_Date LTL1048A	27,903	27,335	95.4	I
Sequence Evolved Gravettian				
Boundary Start Evolved Gravettian	33,007	27,332	95.4	

Table 4b
The sediment composition of the main cultural units.

Archaeological units	Sedimentary facies	Sedimentary composition	Cultural attribution
A-D	FULLY ANTHROPOGENIC DEPOSIT (thickness 2.5–3 m)	Substrate layers heavily altered by human presence representing episodes during which deposition was not controlled by natural processes. Deposit consist in mixtures of sand and gravel that form units with uneven, indistinct bases and flat tops. It contain a huge number of archaeological materials, rounded out of size-exogenous pebbles and abundant charcoals which are generally related to more or less well-structured hearths set directly on the ground or in an artificial "cuvette".	LATE EPIGRAVETTIAN
E	CHANNELFILL GRAVELLY FACIES ASSOCIATED WITH ANTHROPOGENIC LEVELS (thickness 0.8–0.9 m)	Channelfill gravelly facies which pass laterally into the rockfall deposits facies. Palaeochannels in the lower part of the deposit have a low depth/width ratio and are filled with a gravelly lag overlain by silty sand, attributed to ephemeral flows. The uppermost channel-fill deposits commonly show anthropogenic disturbance. The palaeochannel in the upper part of this unit is slightly deeper (0.35 m), filled with gravelly facies. This unit contains several archaeological layers (E1-E16) some of which associated with well-structured heraths.	EVOLVED TO LATE EPIGRAVETTIAN
F	ANTHROPOGENIC DEPOSIT (thickness 0.3 m)	Archaeological levels (F1-F4) with structured hearths standing within a natural channel. They indicates the occurrence of channel reclamation during the frequentation of the layers F.	EARLY EPIGRAVETTIAN
G-H	FLUVIAL FACIES ASSOCIATED WITH ANTHROPOGENIC LEVELS (thickness 1 m)	Fluvial facies associated with anthropogenic levels (G1-G3; H1-H4) with evidence of well-structured hearths on the top (layers G1-G3). Palaeochannels in this unit are wider and shallower, showing gravelly lags, but filled mainly with silty sand, probably by ephemeral runoff. Deposit consist of sandy silt which commonly bears scattered granules and/or small angular pebbles. In the lower part, predominantly massive character might indicate rapid, non-tractional deposition from turbulent suspension, but is more likely due to anthropogenic disturbance. Scattered cobbles and boulders derived from the cave vault are common.	LATE GRAVETTIAN
I-L	TOP OF THE FLUVIAL DEPOSIT ASSOCIATED WITH ANTHROPOGENIC LEVELS (thickness 0.3 m)	Deposit consisting mainly of lens-shaped bodies of cross-stratified gravel or gravelly sand, up to 20–30 cm thick, with erosional, concave-upward bases and flat or gently convex-upward tops. The clast size varies from fine pebble to medium cobble gravel and ranges from rounded to subangular. Clasts are coated with muddy silt and form a clast supported framework filled with sand and granules. Archaelogical levels (I-I1) at the top of layer I are associated with a hearths.	MIDDLE GRAVETTIAN
M-N	FLUVIAL DEPOSIT (thickness 1 m)	Fluvial facies (gravel or gravelly sand) referring to a stream palaeochannels, trending NE–SW. Imbricated gravels in the channel lag show a palaeotransport direction towards the SW. Coarse-grained overbank deposits occur laterally to the palaeochannel and consist of massive, fine- to medium-pebble gravel that forms tabular beds up to 5 cm thick, with sharp basal and top surfaces. A thin Archaeological level on the top of layer M represent the lowest archaeological unit in the sedimentary succession related to the first human occupation of the cave.	

provide an independent chronological tie point for the Grotta del Romito stratigraphy. However, the detailed radiocarbon chronology of the site, coupled with the geochemical characterisation of this tephra layer, means that in the future it has the potential to provide a well dated tephra isochrone that sits in the important transition between the GS-2 and the onset of GI-1. The relevance of this is discussed in further detail below, with regard to the palaeoenvironmental record within the Grotta del Romito deposits.

5.2. Constraining the time of lateglacial environmental changes at Grotta del Romito

The updated chronology for Grotta del Romito, based on a Bayesian model and the new IntCal13 calibration curve (Reimer et al., 2013), is one of the most detailed models produced for a late Upper Palaeolithic site in southern Europe. The new chronology offers the opportunity to place the existing archaeological data within the regional and local environmental context for the last glacial.

Palaeoenvironmental information associated to the Upper Palaeolithic occupation of the cave has been recently derived from the analysis of micro-mammal assemblages (López-García et al., 2014). We have now transferred the results of this study to the new chronology and compared this to the Greenland Ice core record from the INTIMATE stratigraphy (Fig. 7). Micro-mammal response to Lateglacial climate conditions is expressed by the significant shift towards woodland adapted taxa after the H1 stadial, from ~15,800 cal BP, with an intensification of this signal after 15,000 cal BP on the new IntCal-13 based chronology. At Grotta del Romito this transition occurs clearly between layers D11 (14,317–14,103 cal BP) and D29 (15,756–15,288 cal BP) (Fig. 7). The rapid shift to a peak in woodland dominated taxa is coincident with abrupt transition into GI-1e as recorded in Greenland.

The micro-mammal-derived environmental information is in very good agreement with pollen record from the Lago Grande di Monticchio (LGdM), a highly resolved and well-established record of climate and vegetation changes for the Lateglacial in the southern Italian peninsula (Brauer et al., 2007, Fig. 7). This record derives pollen-based Mesic Woodland taxa and has a chronology based on varve counting and tephrochronology. The varve chronology in this period is consistent with calibrated radiocarbon time and this can be demonstrated through comparison of LGdM varve ages for key well-dated Lateglacial tephra, such as the NYT and the Pomici Principale (PP), that now have composite radiocarbon age models derived through the RESET project (Bronk Ramsey et al., 2015). The varve ages for these tephra in the LGdM chronology are 14,120 ± 710 and 12,180 ± 610 cal BP respectively and compare well with Bayesian radiocarbon age model estimates of

Table 5
ROM-D30 WDS EPMA major element geochemical data and comparative geochemical data from Lateglacial Italian tephra, TM layers from Wulf et al. (2004, 2008) Proximal NYT data from Tomlinson et al. (2012).

SiO2	TiO2	Al2O3	FeO	MnO	MgO	CaO	Na2O	K2O	Total
57.93	0.48	17.90	3.94	0.10	0.89	3.17	3.21	8.86	96.49
57.56	0.53	17.90	3.81	0.09	0.91	3.34	3.22	8.62	95.96
58.94	0.46	17.97	3.58	0.10	0.77	2.98	3.50	8.83	97.12
58.08	0.48	17.92	4.09	0.04	0.96	3.38	2.95	8.92	96.82
59.18	0.47	17.86	3.58	0.12	0.76	2.84	3.61	9.02	97.44
58.24	0.45	18.22	3.89	0.11	0.96	3.17	3.36	9.01	97.40
58.11	0.42	18.06	3.25	0.13	0.77	2.95	3.30	9.02	96.01
55.40	0.51	17.77	5.04	0.08	1.55	4.47	3.24	7.50	95.56
58.97	0.44	18.40	3.61	0.12	0.81	2.97	2.98	9.21	97.51
58.47	0.49	17.72	3.37	0.06	0.77	2.90	3.51	8.97	96.26
59.95	0.37	17.44	3.09	0.09	0.55	2.39	3.09	8.83	95.80
59.01	0.49	18.34	3.82	0.12	0.90	3.16	3.73	8.69	98.25
58.81	0.43	18.11	3.33	0.14	0.76	2.90	3.67	8.85	97.00
57.19	0.46	17.48	3.57	0.13	0.83	3.02	3.34	8.67	94.69
59.23	0.39	18.58	3.45	0.06	0.69	2.87	3.42	9.26	97.94
58.51	0.43	18.11	3.58	0.10	0.80	3.23	3.63	8.63	97.04
57.64	0.56	17.95	4.03	0.16	0.92	3.20	3.21	8.72	96.40
59.56	0.43	18.14	3.20	0.14	0.61	2.65	4.16	8.45	97.35
60.57	0.39	17.84	2.63	0.10	0.45	2.09	4.53	8.55	97.16
59.42	0.48	18.42	3.61	0.12	0.73	2.85	3.84	8.77	98.23
57.74	0.54	17.92	3.61	0.14	0.81	3.02	3.32	9.00	96.10
57.59	0.48	17.75	3.50	0.12	0.79	2.99	3.47	8.87	95.57
58.28	0.47	17.92	3.62	0.12	0.78	2.93	3.18	8.98	96.27
59.15	0.49	18.28	3.82	0.15	0.85	3.01	3.53	9.07	98.35
58.91	0.44	18.15	3.70	0.14	0.76	3.01	3.32	9.13	97.56
59.30	0.49	18.13	3.70	0.00	0.77	3.09	3.56	8.66	97.70
59.69	0.42	18.11	3.06	0.14	0.54	2.52	3.26	9.23	96.97
59.21	0.46	18.34	3.72	0.07	0.85	3.17	3.44	9.24	98.50
57.12	0.37	17.39	3.73	0.15	0.76	2.89	3.14	8.96	94.52
58.62	0.50	17.81	3.83	0.14	0.85	2.99	3.39	9.02	97.15
60.85	0.52	18.70	2.81	0.09	0.54	2.24	3.31	9.01	98.07
56.72	0.42	17.44	3.71	0.14	0.87	2.98	3.49	8.73	94.50
57.95	0.42	17.85	3.67	0.06	0.72	2.87	3.45	8.85	95.85
57.49	0.48	17.64	3.96	0.12	1.04	3.39	3.38	8.69	96.19
57.95	0.51	17.36	3.46	0.08	0.76	2.97	3.38	8.90	95.36
58.31	0.49	18.02	3.97	0.14	0.93	3.37	3.14	8.99	97.36
57.29	0.50	17.88	3.88	0.08	0.92	3.29	2.90	8.85	95.59
58.40	0.52	18.11	3.81	0.13	0.91	3.19	3.35	9.18	97.60
59.07	0.46	18.07	3.57	0.18	0.85	2.97	3.46	8.83	97.47
57.28	0.43	17.57	3.62	0.09	0.83	2.98	3.09	8.84	94.72
57.70	0.41	18.63	3.32	0.16	0.72	2.75	3.43	8.72	95.83
58.12	0.42	17.98	3.53	0.05	0.82	3.02	3.01	9.04	95.99
57.95	0.47	17.95	3.70	0.15	0.85	2.96	3.34	8.80	96.18
61.92	0.38	18.33	2.63	0.09	0.32	2.08	4.56	8.26	98.56
58.28	0.48	18.07	3.60	0.04	0.86	3.12	3.35	9.29	97.08
58.88	0.50	18.18	3.50	0.11	0.78	2.93	3.40	9.01	97.29
58.32	0.44	17.85	3.53	0.12	0.81	2.98	3.14	9.18	96.37
57.65	0.48	17.77	3.52	0.09	0.86	2.94	2.99	8.88	95.18
58.44	0.45	18.00	3.90	0.18	0.88	3.34	3.32	9.07	97.59
57.70	0.39	17.68	3.66	0.19	0.88	3.12	3.03	9.01	95.66
58.27	0.50	17.68	3.83	0.09	0.80	3.00	3.24	8.84	96.25
58.60	0.48	17.99	3.46	0.10	0.77	2.83	3.63	8.80	96.65
58.91	0.50	18.19	3.57	0.13	0.76	2.85	3.58	8.91	97.40
57.81	0.46	17.83	3.37	0.16	0.78	2.87	3.17	8.83	95.28
58.19	0.52	17.92	3.73	0.17	0.83	3.07	3.16	9.01	96.61
59.18	0.43	18.22	3.62	0.10	0.90	3.04	3.25	8.98	97.72
58.55	0.45	18.27	3.90	0.04	0.91	3.13	3.23	9.10	97.58
58.11	0.51	17.91	3.91	0.03	0.94	3.40	3.36	8.84	97.00
58.40	0.39	17.58	3.27	0.06	0.74	2.80	3.58	8.69	95.50
58.07	0.48	17.30	3.59	0.04	0.69	2.78	3.21	9.01	95.17
58.86	0.34	18.41	2.80	0.16	0.61	2.68	3.03	9.53	96.42
58.56	0.47	17.69	3.57	0.11	0.78	2.91	3.39	8.89	96.37
58.69	0.48	18.15	3.92	0.09	0.84	3.20	3.34	8.90	97.61
58.62	0.46	17.89	3.64	0.16	0.82	2.94	3.39	9.08	97.00
58.44	0.49	17.83	3.69	0.16	0.83	3.02	3.43	9.20	97.08
57.40	0.45	17.61	3.49	0.07	0.76	2.91	3.35	8.77	94.81
57.90	0.44	17.74	3.55	0.10	0.83	2.94	3.35	8.75	95.60
59.28	0.43	18.13	3.55	0.14	0.72	2.92	3.75	9.10	98.01
58.35	0.45	17.75	3.64	0.12	0.78	2.90	3.12	8.96	96.06
58.51	0.47	18.07	4.00	0.14	0.91	3.03	3.61	8.95	97.69
58.13	0.47	18.27	3.98	0.10	0.94	3.30	3.41	9.00	97.60
57.63	0.49	17.81	3.78	0.08	0.87	3.16	3.34	8.89	96.04

Table 5 (*continued*)

SiO2	TiO2	Al2O3	FeO	MnO	MgO	CaO	Na2O	K2O	Total
59.04	0.42	18.28	3.66	0.10	0.82	2.93	3.68	8.86	97.80
58.66	0.41	18.02	3.67	0.14	0.86	3.09	3.24	8.99	97.07
58.36	0.47	17.90	4.01	0.16	0.86	3.25	3.31	9.10	97.43
58.32	0.50	18.17	3.89	0.15	0.87	3.05	3.48	9.19	97.62
58.08	0.44	17.83	3.89	0.04	0.95	3.27	3.35	9.09	96.94
57.61	0.45	19.09	3.71	0.17	0.81	3.07	3.17	9.00	97.08
58.85	0.39	18.27	3.54	0.11	0.73	3.02	3.36	9.04	97.32
58.86	0.48	18.25	3.66	0.13	0.75	3.01	3.71	8.95	97.79
57.83	0.45	17.72	3.56	0.07	0.77	2.90	3.28	9.00	95.58
57.52	0.44	18.02	3.62	0.10	0.77	2.89	3.09	9.01	95.46
59.41	0.43	18.83	3.01	0.11	0.58	2.70	3.40	9.56	98.03
58.29	0.46	17.91	3.92	0.18	0.88	3.05	3.32	9.02	97.01
57.80	0.41	17.75	3.53	0.11	0.90	3.09	3.23	8.82	95.64
57.82	0.49	18.07	3.53	0.09	0.91	3.09	3.30	9.01	96.32
58.52	0.41	17.96	3.64	0.15	0.77	2.78	3.25	9.16	96.65
58.84	0.46	18.16	3.36	0.16	0.69	2.81	3.59	8.71	96.79
57.81	0.43	17.80	3.83	0.09	0.88	3.01	3.49	8.55	95.89
59.09	0.46	18.17	3.84	0.19	0.84	3.03	3.41	8.99	98.02
59.20	0.48	18.55	3.75	0.14	0.86	3.10	3.56	8.90	98.55
58.17	0.44	18.09	3.80	0.16	0.82	3.07	3.42	9.07	97.04
60.99	0.40	18.20	2.61	0.24	0.37	2.01	4.68	8.32	97.82
59.11	0.48	18.13	3.52	0.08	0.80	2.77	3.51	9.09	97.50
58.79	0.43	18.21	3.47	0.14	0.80	3.05	3.05	9.10	97.04
57.96	0.54	17.94	4.32	0.15	0.98	3.30	3.15	8.94	97.28
58.93	0.41	18.57	3.85	0.21	0.88	3.15	3.23	9.07	98.30
58.52	0.43	18.06	3.71	0.10	0.85	3.12	3.22	9.14	97.17
60.22	0.37	17.98	2.56	0.10	0.38	1.99	4.34	8.38	96.31
58.04	0.58	18.17	3.96	0.08	0.91	3.28	3.32	9.19	97.52
57.43	0.50	17.67	3.18	0.08	0.70	2.64	3.66	8.59	94.45
58.62	0.44	18.29	3.42	0.12	0.77	3.01	3.36	8.92	96.96
57.48	0.45	18.15	3.87	0.08	0.85	2.96	3.36	8.93	96.12
58.06	0.43	17.74	3.14	0.10	0.67	2.66	3.69	8.37	94.85
58.59	0.43	18.38	3.67	0.13	0.84	3.03	3.37	9.16	97.59
58.76	0.46	17.80	2.63	0.19	0.32	2.00	4.29	8.22	94.67
58.18	0.46	18.16	3.78	0.12	0.82	3.01	3.29	9.14	96.96
57.89	0.47	17.89	3.75	0.16	0.98	3.21	3.04	8.96	96.37
60.26	0.33	17.84	2.61	0.16	0.37	2.05	4.65	8.45	96.71
58.28	0.40	17.90	3.67	0.04	0.79	2.92	3.35	9.12	96.48
58.72	0.45	17.97	3.47	0.06	0.85	2.99	3.36	9.14	97.01
58.77	0.55	18.18	3.67	0.17	0.84	3.00	3.62	9.18	97.98
60.92	0.43	18.09	2.62	0.15	0.41	2.15	4.65	8.13	97.56
61.26	0.41	18.32	2.41	0.20	0.32	2.06	4.48	8.60	98.06
58.35	0.49	17.92	3.63	0.20	0.81	2.99	3.48	9.22	97.07
58.62	0.48	18.08	3.78	0.08	0.87	2.94	3.27	9.18	97.28
59.21	0.41	18.16	3.64	0.13	0.66	2.91	3.62	8.82	97.56
63.85	0.30	18.09	1.75	0.13	0.11	1.52	5.56	6.63	97.93
57.21	0.46	17.68	3.57	0.10	0.89	3.00	3.30	9.01	95.22
59.06	0.49	18.05	3.46	0.12	0.72	2.85	3.58	9.05	97.39
58.96	0.53	18.12	3.81	0.12	0.89	3.25	3.56	8.96	98.21
58.68	0.47	17.85	3.96	0.18	0.91	3.11	3.42	8.45	97.03
57.96	0.47	18.12	3.77	0.13	0.96	3.32	3.34	9.20	97.27
63.23	0.38	17.28	2.42	0.26	0.16	1.44	6.18	6.16	97.51
58.44	0.47	18.15	3.82	0.15	0.78	3.10	3.12	9.02	97.06
57.90	0.48	18.16	3.78	0.18	0.91	3.06	3.13	8.82	96.42
58.76	0.51	17.87	3.81	0.03	0.79	3.02	3.42	9.05	97.26
57.96	0.54	17.93	4.06	0.16	0.97	3.17	3.15	8.84	96.78
58.46	0.47	18.06	3.74	0.01	0.92	3.10	3.33	9.18	97.29
59.22	0.47	18.23	3.71	0.10	0.88	3.18	3.61	8.55	97.95
61.05	0.45	18.04	2.65	0.03	0.40	2.10	4.52	8.32	97.56
58.22	0.45	18.01	3.84	0.09	0.90	3.21	3.10	9.05	96.86
58.70	0.42	18.02	4.25	0.25	0.91	3.17	3.69	8.55	97.96
58.72	0.47	18.15	3.66	0.14	0.77	2.98	3.66	9.15	97.70
58.98	0.51	18.03	3.60	0.12	0.78	3.07	3.53	9.06	97.69
61.37	0.42	18.28	2.70	0.15	0.45	2.13	3.95	8.50	97.96

14,588–13,884 cal BP for the NYT and 12,091 - 11,850 cal BP for the PP. The LGdM data are also reported in Fig. 7 and a percentage Mesic Woodland pollen is reported in the LGdM chronology from the Brauer et al. (2007) record. A direct comparison of environmental information derived from micro-mammals from Grotta del Romito and pollen data from LGdM shows a clear covariance. At Grotta del Romito, the timing of the transition from dry to wooded taxa species is synchronous to the shift from steppe environments

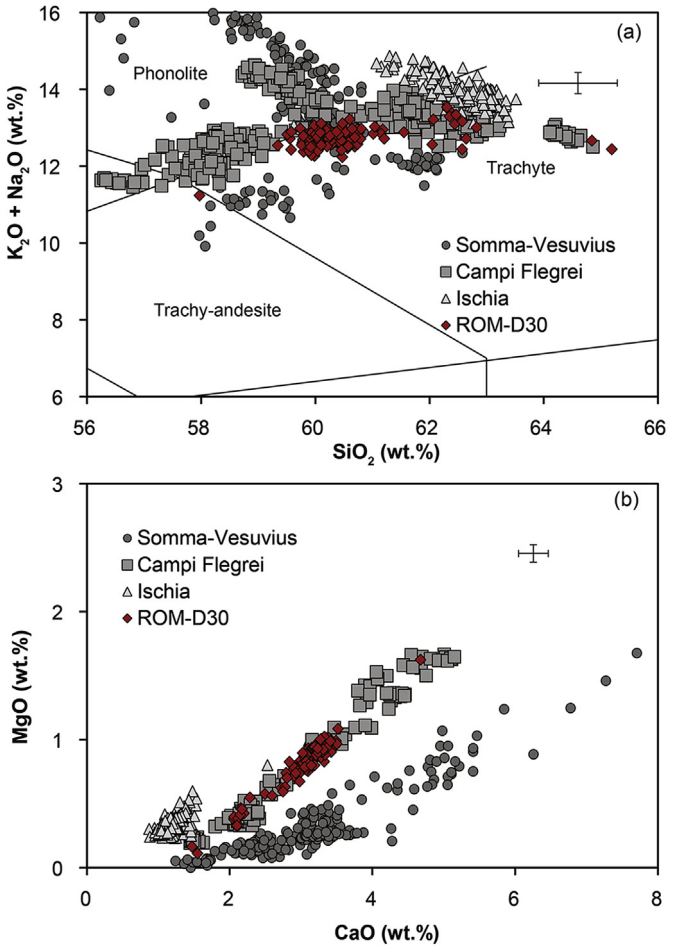

Fig. 5. Total Alkali versus Silica plot (>56 wt % SiO2; TAS; Le Bas 1986) (5a) and CaO vs MgO (5b), for the ROM-D30 tephra and composite data from the Campi Flegrei; Somma Vesuvius and Ischia volcanic provinces (reference data from Tomlinson et al., 2012, 2014; 2015).

towards wooded environments after ~15,000 cal BP in LGdM. These correspondences confirm that Lateglacial environmental conditions at Grotta del Romito were sensitive to regional and hemispheric centennial-millenial-scale changes in climate.

Evidence of regional atmospheric changes during the Lateglacial at Grotta del Romito is also offered by the oxygen isotope composition of land snail shells recovered from late Epigravettian units (Colonese et al., 2007), placed on the revised chronology and compared to Greenland Ice Core data (Fig. 8). These cover a period from ~14,300 to ~13,000 cal BP on the revised chronology and span most of the Lateglacial interstadial, which is broadly correlated to the warm but unstable GI-1 interstadial from the Greenland records. Fig. 8 is a comparison of the snail shell $\delta^{18}O$ (‰ V-PDB) values with the $\delta^{18}O$ (‰ V-SMOW) palaeoclimate reconstructions from the NGRIP ice core on the GICC05 timescale, with the sub stages of GI-1 from the INTIMATE event stratigraphy (Rasmussen et al., 2014). While it is clear that the sampling resolution of the Grotta del Romito data does not capture all of the subtleties expressed in the Greenland record, there is broad similarity between the expressions of the interstadial in both archives. In particular, there is a clear correspondence in both records of the abrupt isotopic shifts from the warm GI-1e early interstadial through the GI-1d reversal and back into warmer conditions in GI-1c. This relationship between Grotta del Romito and Greenland had been suggested before (Colonese et al., 2007), however this was constrained due to the comparison to only one ice core (GISP2) and chronological discrepancies between different ice core records for the timing of the GI events between the GISP2 and GRIP ice cores (Rasmussen et al., 2006). This has been resolved with the development of GICC05 and the integration of the different ice core timescales using volcanic markers. The integrated GICC05 age of the GI-d event is 14,025 ± 169 years BP (converted from b2k by subtracting 50 years) and this closely matches the mid-point of the Grotta del Romito isotope excursion dated in the revised chronology to 14,217–14,016 cal BP. The shift in isotope values in the Grotta del Romito record is significant and it is not yet clear if this can all be equated to a change in temperature recorded in meteoric water (Colonese et al., 2007), however, the revision to both the Grotta del Romito chronology and the development of GICC05 now make the chronological equivalence to GI-1d clear. Further work on the isotopic composition of a range of faunal material is now underway, based on this new chronostratgraphic framework.

5.3. Human response to lateglacial climate and environmental conditions at Grotta del Romito

The revised chronology allows us to constrain the timing of human occupation at Grotta del Romito during the last Lateglacial and to explore its broad socio-economic and cultural implications. Using the model set to calculate the transitions between different cultural phases and estimate their spans we can examine the different cultural units within the cave. Table 4 shows the output of this version of the model. The data is not particularly useful for the Evolved Gravettian as there is only one available date, however from the transition between the Evolved and Late Gravettian onward it is possible to calculate the timing of the boundaries between the cultural phases and the spans of these. The significance of some of these transitions is discussed below.

The sampling strategy at the site was to date archaeological sub-layers where possible. The numbers of individual radiocarbon analyses taken for each of the main units is a reflection of the archaeological activity through time at the site, as sub-layers in the site stratigraphy are denoted on archaeological grounds with the appearance of activity surfaces. In some cases, sub-layers have several dates on a layer and this also, in part, reflects activity and the presence of datable hearth units within a sub-layer. Thus, while not a perfect measure a greater number of dated samples in a particular layer represents evidence of increased human activity at the site.

Using the main age model from Table 2 the first secure evidence of human occupation (Fig. 9a and b) can now be constrained at least between 28,003–26,958 and 25,488–23,713 cal BP (layers I to H4, layer M with archaeological remains is not dated), and are represented by few archaeological remains (lithic and faunal) corresponding to the end of the Evolved Gravettian (Martini and Lo Vetro, 2005a; Martini et al., 2015). The occupation seems to have been sporadic at that time, in part due to major episode of strong water runoff within the cave (Ghinassi et al., 2009), when climate was wetter and colder in the southern Italian Peninsula (e.g. Giraudi, 1989; Ramrath et al., 1999). Large mammal remains exploited as food source are also very scarce (Bertini Vacca, 2012), and are dominated by ibex (*Capra ibex*; 73%). Today this species inhabits high altitude, steep slope environments, thus it is likely to be indicative of hunting activities predominantly in open environments.

An increase in human occupation occurs between 23,609 and 23,058 and 21,365–20,638 cal BP (layers G2 to F1), during the LGM (Martini and Lo Vetro, 2005a,b). This time interval is represented by the thickest anthropogenically modified deposit at the bottom of the succession (Ghinassi et al., 2009), and include lithic and faunal

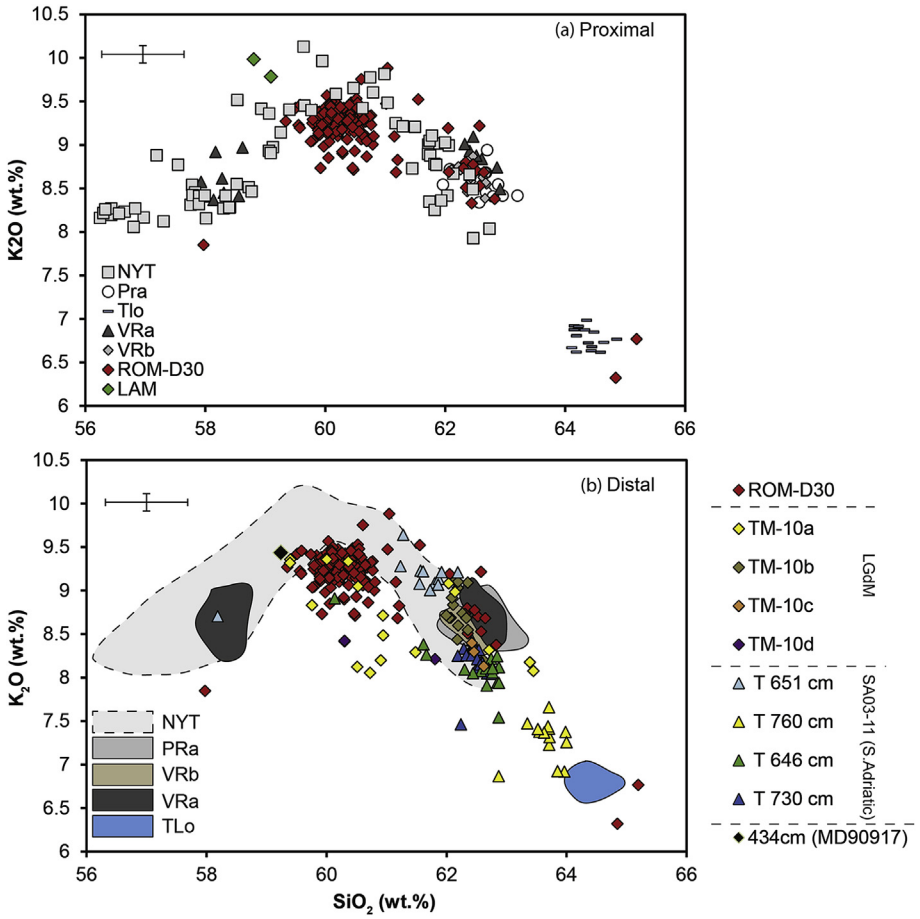

Fig. 6. SiO2 vs K2O plots for the ROM-D30 tephra against (6a) the Tufi Biancastri eruptive succession between the Campanian Ignimbrite (CI) and the NYT (Orsi et al., 1996). In particular the K-trachytic glasses which were repeatedly erupted at CF caldera during this post-CI and Pre-NYT period (e.g., eruptive units PRa, VRa, VRb; Tomlinson et al., 2012). The ROM-D30 data is also compared to tephra recorded in downwind archives (6b) of Lago Grande di Monticchio (LGdM; Wulf et al., 2008), and two Adriatic marine cores (MD90917; Siani et al., 2004; SA03-11; Matthews et al., 2015).

remains, as well as structured fireplaces attributable to the Late Gravettian and the Early Epigravettian (Martini and Lo Vetro, 2005a,b; Martini et al., 2012). The Late Gravettian spans 265–1776 cal years and the Early Epigravettian spans 1221–1925 cal years. Ibex continued to be the main target species (65%), although a considerable increase of chamois (*Rupicapra* sp.) from 23,540–22,910 to 19,848–18,943 cal BP (Bertini Vacca, 2012) points to some changes in local/regional environmental conditions. Chamois is a cold-adapted mountain-dwelling species (Corlatti et al., 2011) and along with ibex possibly indicate decreasing temperatures and expansion of open environments during this time interval. This ecological scenario is in broad agreement with the expansion of Mesic woody Taxa for the key regional record from Lago Monticchio (Fig. 9a), taken from Brauer et al. (2007).

Increased human occupation at Grotta del Romito between 23,609 and 23058 and 21,365–20,638 cal BP may have been favoured by reduced water runoff during dry conditions of the LGM (RM2c in Ghinassi et al., 2009). However, it also corresponds to an interval of unprecedented demographic changes in southern Europe. The LGM is considered the most dramatic climate event experienced by anatomically modern humans (Brewster et al., 2014). The establishment of full glacial conditions, with decreasing surface temperatures by 8–15 °C compared to present day (Heyman et al., 2013/1), favoured the expansion of ice sheets to middle and north regions of the continent, forcing a large part of human population to move south, toward Mediterranean and Atlantic boards of Europe (Gamble et al., 2004). Such unique demographic reorganization is expressed by the increasing number of Upper Palaeolithic sites in southern France (Bocquet-Appel et al., 2005; French and Collins 2015/3; Tallavaara et al., 2015), in Iberian and possibly also in Italian Peninsula (Straus, 1991, 2005). More recently, palaeogenetic studies have shown significant population changes among European hunter-gatherers as the result of their large-scale contraction and expansion from southern refugia (Iberian and Italian Peninsulas) before and after the LGM (Gamble et al., 2004; Torroni et al., 2001; Fu et al., 2016; Posth et al., 2016). This phase at Grotta del Romito also corresponds with the cultural transition from the Late Gravettian (Layer G) to the Early Epigravettian (Layer F). This transition is substantially represented by innovations in the lithic assemblages with components originated from northwest areas of the Pensinsula (Martini and Lo Vetro, 2005b). The intensified occupation of Grotta del Romito between 23,609–23,058 and 21,365-20,638cal BP (sub-layers G2 to F1), thus, might be indicative of changing settlement pattern and more frequent use of the cave during an interval of crucial demographic and cultural changes in southern Europe and Italian Peninsula.

The cave continues to be occupied during the onset of the deglaciation (Fig. 9), with several isolated events chronologically constrained between 19,848–18,943 and 16,749–15,943 cal BP (layer E), and represented by distinct levels (sub-layers E16-E1) containing lithic and faunal remains, fireplaces and pits culturally associated to the Evolved Epigravettian and the first part of the

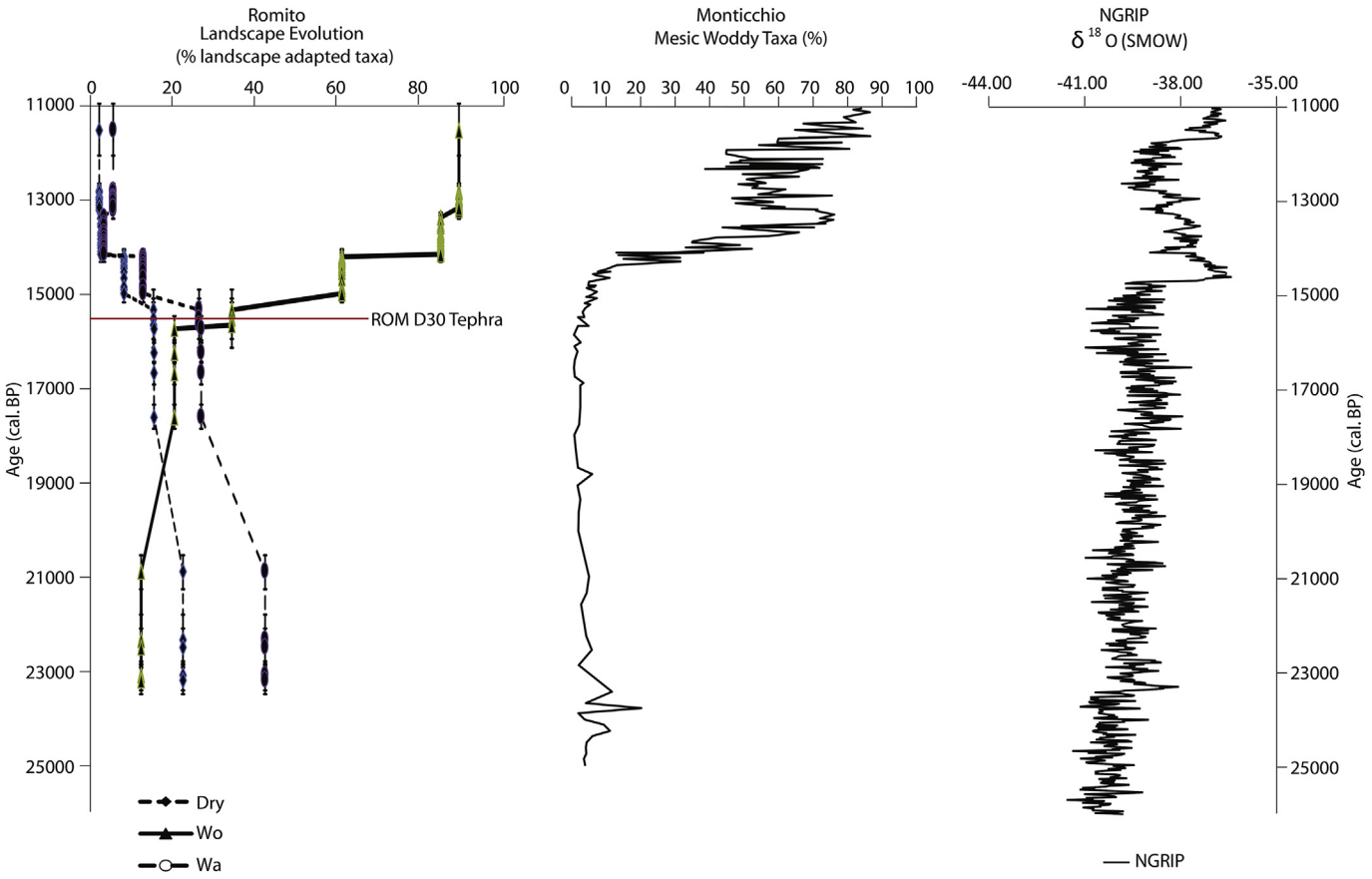

Fig. 7. Micro-mammal percentages grouped by habitat preferences Dry and their inferred landscape preferences (Dry, Woodland (Wo) and Water (Wa); López-García et al., 2014) on the revised Bayesian timescale compared to the LGdM pollen record of Brauer et al. (2007) and the NGRIP ice core record on the GICC05 chronology (Rasmussen et al., 2006, 2014). Also shown is the age and stratigraphic position of the ROM-D30 tephra in relation to the landscape data.

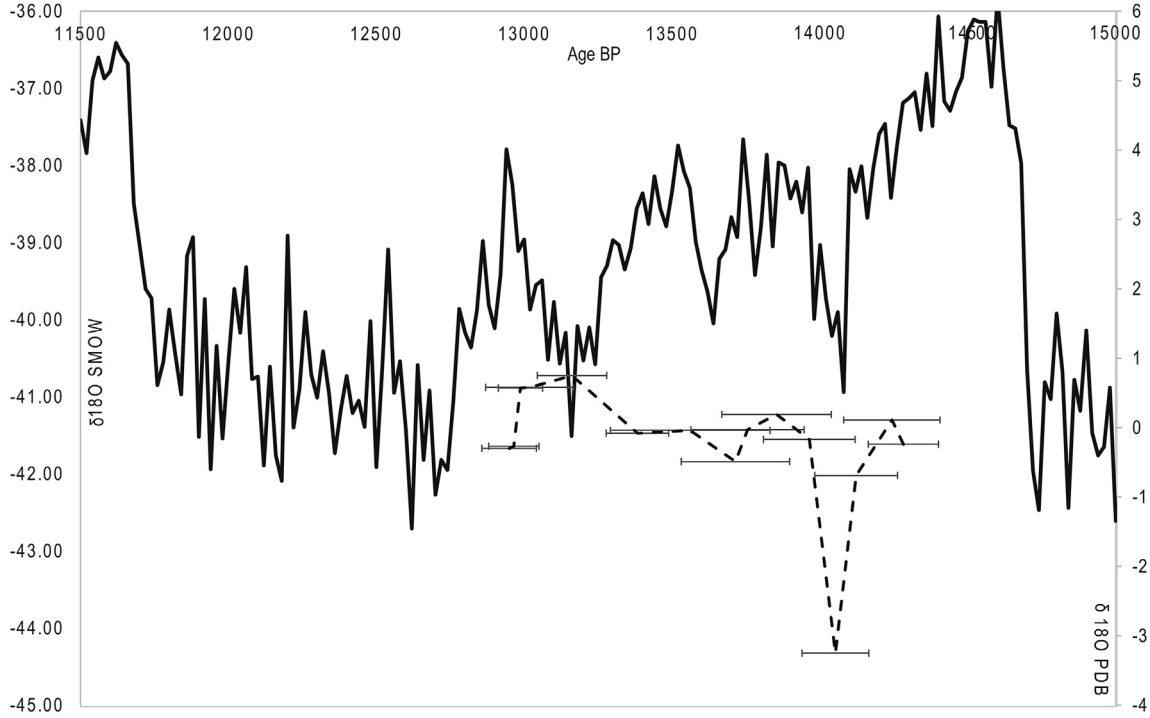

Fig. 8. Romito $\delta^{18}O$ values from terrestrial molluscan shells (Colonese et al., 2007) on the revised Bayesian timescale (dashed lines) compared to the NGRIP ice core record on the GICC05 chronology (Rasmussen et al., 2006, 2014).

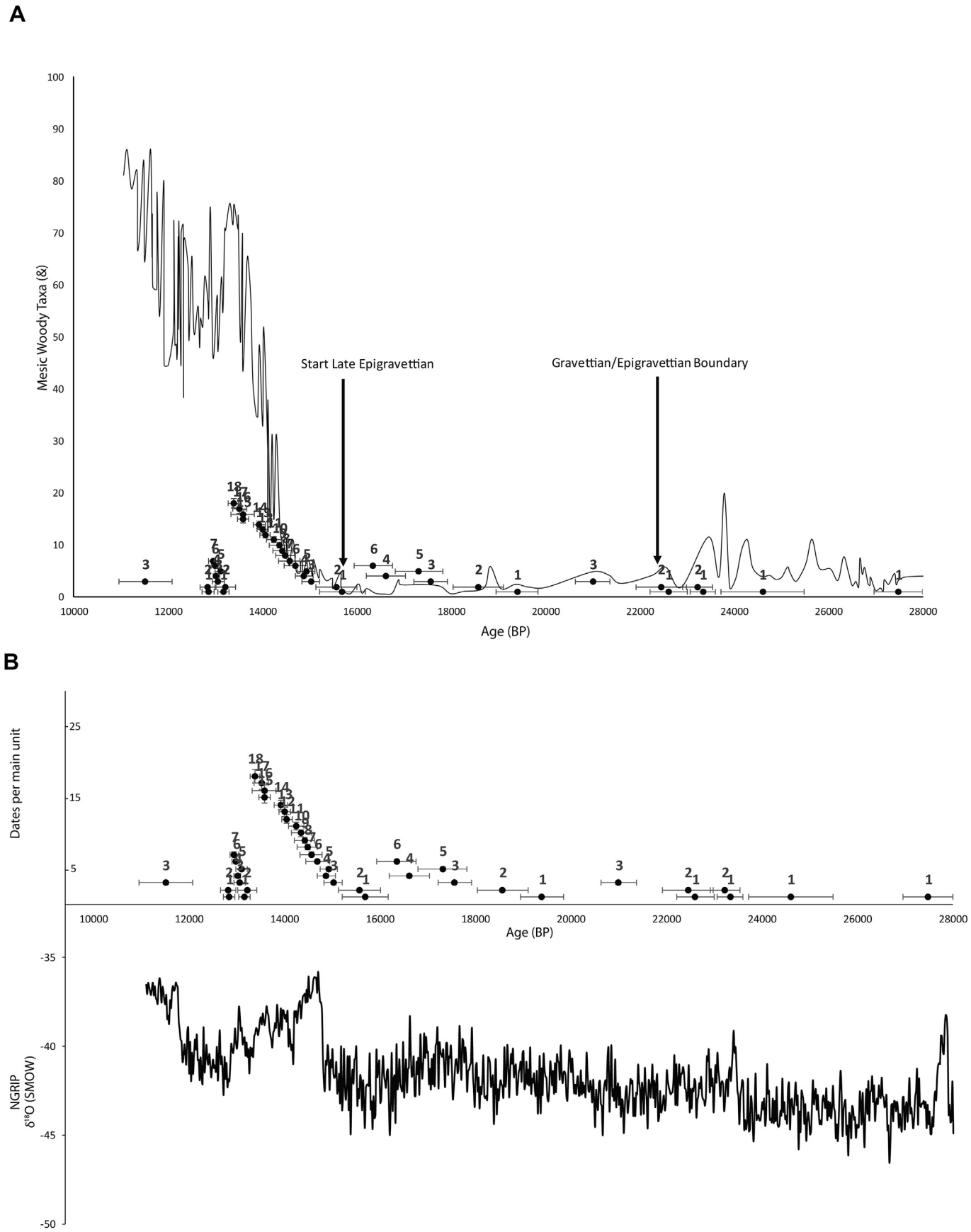

Fig. 9. a) Romito dates reported as the number of dates within archaeological layers H (oldest) to B (youngest) in this study, as a proxy for archaeologically observed human occupation, reported against Mesic Woody taxa from LGdM from Brauer et al. (2007); b) Romito dates reported as the number of dates within archaeological layers H (oldest) to B (youngest) reported against and NGRIP ice core $\delta^{18}O$ on the GICC05 timescale (Rasmussen et al., 2006, 2014).

Final Epigravettian. The fauna is again dominated by ibex (80%), while chamois decrease to the lowest values of the succession (7%). This time interval corresponds with the H1 stadial and the regional palaeoclimatic records pointing to open environments with sparse or restricted tree cover (Huntley et al., 1999), which is locally confirmed by the micro-mammal assemblages (López-García et al., 2014). The large mammal assemblages also support this scenario, although a decrease in chamois could indicate that conditions were not as cold and dry as the phase before. The sedimentary record from these levels shows evidence for increased water runoff (Ghinassi et al., 2009), which may reflect wetter conditions compared to the LGM, or at least an increase in flooding frequency.

The Lateglacial marks a key turning point in human use of Grotta del Romito. Human occupation intensifies progressively from ~16,025 cal BP (layers D35), and reach unprecedented levels between 15,756 and 12,970 cal BP (layers D29 and C; Fig. 9a), as attested by the abundance of faunal and artefacts remains, fireplaces and pits along with several intact human burials (Colonese and Martini, 2007; Martini et al., 2007, 2012; Craig et al., 2010; Bertini Vacca et al., 2012). The significant intensification of the occupation of Grotta del Romito is clear in Fig. 9a, where the numbers of dates within the archaeological units is shown against local palaeoenvironmental indicators. These suggest a sustained and rapid increase in occupation of the cave closely linked to ameliorating local conditions. Fig. 9a shows the detail of this intensification of occupation of the cave in the Lateglacial with a significant increase in the number of archaeological dates between ~15,000 and 13,000 cal BP. This period of intensification corresponds to the Late Epigravettian, which is the cultural unit associated with the whole Lateglacial period and has a span of 3543–4348 calendar years (95.4% CI). The Evolved/Late Epigravettian boundary at 16,375-15549 cal BP is chronologically coincident with the first increase in woody taxa (Fig's 9a-b) and the significant rise in the archaeological levels in the cave, taken here as a proxy for the intensity of human presence, is synchronous with the dramatic increase in woody taxa from ~14,300–13,000 cal BP.

The climatic context of this is also clearly shown in Fig. 9b which compares the Grotta del Romito archaeological data to regional palaeoclimate data from from the Greenland NGRIP ice core using the GICC05 chronology (Rasmussen et al., 2014). These data clearly suggest that the major demographic transition at Grotta del Romito is linked to abrupt regional scale climate change. It is possible that the ameliorating environmental conditions during the deglaciation favoured a more intensive occupation, perhaps as response to increased population density and territoriality.

During this expansion in occupation of Grotta del Romito faunal remains reveal a much more diversified set of resources, with ibex showing relative proportions similar to wild boar, followed by red deer, chamois and roe deer. This biodiversity likely reflects the existence of distinct ecological niches and increasing vegetation cover. This is locally supported by the increasing diversity of terrestrial gastropods and micro-mammals (Colonese and Martini, 2007; López-García et al., 2014), and regionally corroborated by the progressive increase in arboreal pollens, humidity and winter temperatures at the LGdM (Huntley et al., 1999), Fig. 9b. It is worth noting that ROM-D30 tephra dated to 15,817–14,933 cal BP lies immediately below this new cultural and environmental interval at Grotta del Romito (layer D30). Thus, its stratigraphic position, as well as its reported age, makes it a potential new marker for the onset of the Lateglacial interstadial in the central Mediterranean basin.

5.4. Wider significance

While this is a site specific study, the results of revaluating the chronology of the Grotta del Romito record suggest that human occupation and biodiversity recorded at the site are closely coupled to wider scale climatic and environmental changes. These are also coincident with broader demographic changes across Europe. While there are a number of other central Mediterranean sites that may also show these changes, very few have the level of chronological detail required to be able to evaluate the demographic and archaeological changes at the resolution required to test the link between human adaptation and abrupt climate forcing. It is clear from Grotta del Romito, however, that with sufficient chronological control and the detailed linking of archaeological, *in situ* biological data and wider climate records that it is possible to evaluate the influence of changing climates on human populations during the Last Glacial in southern Europe.

Relatively few studies have considered the detail of the impact of Abrupt Lateglacial climate change on human populations in Southern Europe up to this point at this level of detail. However large database studies of the recolonization of Northern Europe from the refugia zones have been undertaken in a number of regions (Housley et al., 1997; Gamble et al., 2004, 2005; Blockley et al., 2006; Jacobi and Higham, 2009). On the basis of a compilation of a large database of radiocarbon dates Gamble et al. (2005) have proposed initial population expansion in Iberia and southern France as early as 19,000 cal BP, and certainly prior to warming recorded in Greenland. They suggest, however, that the main demographic expansion in both these regions is between 16,000–13,000 cal BP before further contraction in the Younger Dryas, after 12,900 cal BP (regarding the Iberian peninsula see also Aura et al., 2011, about the impact of Younger Dryas on human frequentation in eastern Spain). Unlike the pattern of occupation suggested for Southern France and Iberia, however, the Grotta del Romito record does not show any significant population expansion in the pioneer expansion phase (19,000–16,000) postulated by Gamble et al. (2005). Given that Grotta del Romito is an upland site, this suggests that any demographic expansion in this part of Italy has not reached a level where significant exploitation of upland resources is viable. At the same time the rapid increase in human presence and exploitation of Grotta del Romito between 16,000–13,000 cal BP, coupled with a shift in the local ecology is strikingly in phase with the main population expansions across Iberia and France (Gamble et al., 2004, 2005). Such demographic expansion could also be evidenced in Italy by the growth in number of sites during the Final Epigravettian (Palma di Cesnola, 1993).

6. Conclusion

This study has comprehensively revised the chronology of Grotta del Romito, a crucial Upper Palaeolithic site in southern Europe and in the Mediterranean region. The combination of Bayesian age modelling, calibration with the IntCal-13 curve (Reimer et al., 2013), and the application of tephrochronology have allowed us to build on the existing work at this site. The revised Grotta del Romito chronology is now exceptionally robust. This has allowed several key findings. Firstly, we have shown that some of the direct dates on human teeth are stratigraphically consistent with the main radiocarbon record from Grotta del Romito. Secondly, we show that there is significant variation in the levels of human occupation at the site. Thirdly, we have compared the record of archaeological activity with environmental data from within the Grotta del Romito record, using the revised chronology with a range of regional climate indicators. This exercise shows, fourthly, that there is a close correspondence between human occupation of the cave and environmental changes, with a marked increase in occupation during the warming in the Lateglacial period. This is also in accord with wider scale evidence from

Southern France and Iberia, but here we are able to show that is closely correlated with local and regional environments. Finally, we report a new tephra (ROM-D30) that is stratigraphically at the start of the shift in both local environment recorded in the cave and the significant increase in human presence. We have reported on the age and chemistry of this tephra layer and show that it cannot be linked to known widespread tephra and thus it may become a new and important regional marker in future studies.

Acknowledgements

This research was supported by a grant from the Leverhulme Trust (F/0 0235/I) and by a Natural Environment Research Council ORADS radiocarbon dating award (NF/2011/2/7). We are also grateful for the helpful comments from Giovanni Zanchetta and an additional anonymous referee.

Appendix A. Supplementary data

Supplementary data related to this article can be found at https://doi.org/10.1016/j.quascirev.2017.09.007.

References

Albert, P.G., Tomlinson, E., Lane, C.S., Wulf, S., Smith, V.C., Coltelli, M., Keller, J., Lo Castro, D., Manning, C.J., Müller, W., Menzies, M.A., 2013. Lateglacial explosive activity on Mount Etna: implications for proximal-distal tephra correlations and the synchronization of Mediterranean archives. J. Volcanol. Geotherm. Res. 265, 9–26.

Allen, J.R.M., Brandt, U., Brauer, A., Hubberten, H.-W., Huntley, B., Keller, J., Kraml, M., Mackensen, A., Mingram, J., Negendank, J.F.W., Nowaczyk, N.R., Oberhänsli, H., Watts, W.A., Wulf, S., Zolitschka, B., 1999. Rapid environmental changes in southern Europe during the last glacial period. Nature 400 (6746), 740–743.

Aura, J.E., Jordá, J.F., Montes, L., Utrilla, P., et al., 2011. Human responses to younger Dryas in the Ebro valley and mediterraneanwatershed (Eastern Spain). Quat. Int. 242, 348–359.

Bar-Matthews, M., Ayalon, A., Kaufman, A., Wasserburg, G.J., 1999. The Eastern Mediterranean paleoclimate as a reflection of regional events: Soreq cave, Israel. Earth Planet. Sci. Lett. 166, 85–95.

Barker, G.W.W., 1981. Landscape and Society: Prehistoric Central Italy. Academic Press, London.

Bertini Vacca, B., 2012. The hunting of large mammals in the upper palaeolithic of southern Italy: a diachronic case study from Grotta del Romito. Quat. Int. 252, 155–164.

Bertini Vacca, B., Di Giuseppe, Z., De Curtis, O., Lo Vetro, D., Martini, F., Nannini, L., Trenti, F., Sala, B., 2012. Uomo, clima e ambiente in Calabria nel II Pleniglaciale: nuovi dati da Grotta del Romito (CS). In: De Grossi Mazzorin, J., Saccà, D., Tozzi, C. (Eds.), Atti del 6° Convegno Nazionale di Archeozoologia, Parco dell'Orecchiella, 21–24 maggio 2009, San Romano in Garfagnana – Lucca, AIAZ, 63-69.

Blockley, S.P.E., Lowe, J.J., Walker, J.J., Asioli, A., Trincardi, F., Coope, G.R., Donahue, R.E., Pollard, A.M., 2004. Bayesian analysis of radiocarbon chronologies: examples from the European Lateglacial. J. Quat. Sci. 19, 159–175.

Blockley, S.P.E., Blockley, S.M., Donahue, R.E., Lane, C.S., Lowe, J.J., Pollard, A.M., 2006. The chronology of abrupt climate change and Late Upper Palaeolithic human adaptation in Europe. J. Quat. Sci. 21, 575–584.

Blockley, S.P.E., Ramsey, C.B., Lane, C.S., Lotter, A.F., 2008. Improved age modelling approaches as exemplified by the revised chronology for the central European varved lake, Soppensee. Quat. Sci. Rev. 27, 61–71.

Bocquet-Appel, J.-P., Demars, P.-Y., Noiret, L., Dobrowsky, D., 2005. Estimates of Upper Palaeolithic meta-population size in Europe from archaeological data. J. Archaeol. Sci. 32, 1656–1668.

Brauer, A., Allen, J.R.M., Mingram, J., Dulski, P., Wulf, S., Huntley, B., 2007. Evidence for last interglacial chronology and environmental change from Southern Europe. Proc. Natl. Acad. Sci. U. S. A. (PNAS) 104 (2), 450–455.

Brewster, C., Meiklejohn, C., von Cramon-Taubadel, N., Pinhasi, R., 2014. Craniometric analysis of European upper palaeolithic and mesolithic samples supports discontinuity at the last glacial maximum. Nat. Commun. 5, 4094.

Bronk Ramsey, C., 2008. Deposition models for chronological records. Quat. Sci. Rev. 27, 42–60.

Bronk Ramsey, C., 2009a. Bayesian analysis of radiocarbon dates. Radiocarbon 51, 337–360.

Bronk Ramsey, C., 2009b. Dealing with outliers and offsets in radiocarbon dating. Radiocarbon 51, 1023–1045.

Bronk Ramsey, C., Albert, P.G., Blockley, S.P.E., Hardiman, M., Housley, R.A., Lane, C.S., Lee, S., Matthews, I.P., Smith, V.C., Lowe, J.J., 2015. Improved age estimates for key late quaternary European tephra horizons in the RESET lattice. Quat. Sci. Rev. 118, 18–32.

Buck, C.E., Kenworthy, J.B., Litton, C.D., Smith, A.F.M., 1991. Combining archaeological and radiocarbon information - a Bayesian-approach to calibration. Antiquity 65, 808–821.

Candy, I., Adamson, K., Gallant, C.E., Whitfield, E., Pope, R., 2012. Oxygen and carbon isotopic composition of quaternary meteoric carbonates from western and southern Europe: their role in palaoenvironmental reconstruction. Palaeogeogr. Palaeoclimatol. Palaeoecol. 326–328, 1–11.

Clark-Balzan, L.A., Candy, I., Schwenninger, J.-L., Bouzouggar, A., Blockley, S., Nathan, R., Barton, R.N.E., 2012. Coupled U-series and OSL dating of a late Pleistocene cave sediment sequence, Morocco, North Africa: significance for constructing palaeolithic chronologies. Quat. Geochronol. 12, 53–64.

Colonese, A.C., Martini, F., 2007. Molluschi terrestri e disturbi antropici: evidenze epigravettiane a Grotta del Romito (Cosenza). Bull. Paletnol. Ital. 96, 1–15.

Colonese, A.C., Zanchetta, G., Fallick, A.E., Martini, F., Manganelli, G., Lo Vetro, D., 2007. Stable isotope composition of Lateglacial land snail shells from Grotta del Romito (Southern Italy): palaeoclimatic implications. Palaeogeogr. Palaeoclimatol. Palaeoecol. 254, 550–560.

Corlatti, L., Lorenzini, R., Lovari, S., 2011. The conservation of the chamois Rupicapra spp. Mamm. Rev. 41, 163–174.

Craig, O., Biazzo, M., Colonese, A.C., Di Giuseppe, Z., Martinez-Labarga, C., Lo Vetro, D., Lelli, R., Martini, F., Rickards, O., 2010. Stable isotope analysis of late upper palaeolithic human and faunal remains from Grotta del Romito (Cosenza), Italy. J. Archaeol. Sci. 30, 1–9.

De Silva, M., Pizziolo, G., Lo Vetro, D., De Troia, V., Machetti, P., Ortisi, F.E., Martini, F., 2016. Ritual use of Romito cave during the late upper palaeolithic: an integrated approach for spatial reconstruction. In: Campana, S., Scopigno, R., Carpentiero, G., Cirillo, M. (Eds.), Proceedings of the 43rd Computer Applications and Quantitative Methods in Archaeology, CAA Conference 2015, "Keep the Revolution Going", 30 March- 3 April 2015, Siena, Archaeopress Archaeology, vol. 1, pp. 685–698.

Fabbri, P.F., Graziosi, P., Guerri, M., Mallegni, F., 1989. Les hommes des sépoltures de la grotte du Romito à Papsidero (Cosenza, Italie). In: Giacobini, G. (Ed.), Hominidae, Proceedings of the 2nd International Congress of Human Paleontology, Milan, pp. 487–494.

French, J.C., Collins, C., 2015/3. Upper Palaeolithic population histories of Southwestern France: a comparison of the demographic signatures of 14C date distributions and archaeological site counts. J. Archaeol. Sci. 55, 122–134.

Fu, Q., Posth, C., Hajdinjak, M., Petr, M., Mallick, S., Fernandes, D., Furtwängler, A., Haak, W., Meyer, M., Mittnik, A., Nickel, B., Peltzer, A., Rohland, N., Slon, V., Talamo, S., Lazaridis, I., Lipson, M., Mathieson, I., Schiffels, S., Skoglund, P., Derevianko, A.P., Drozdov, N., Slavinsky, V., Tsybankov, A., Cremonesi, R.G., Mallegni, F., Gély, B., Vacca, E., Morales, M.R.G., Straus, L.G., Neugebauer-Maresch, C., Teschler-Nicola, M., Constantin, S., Moldovan, O.T., Benazzi, S., Peresani, M., Coppola, D., Lari, M., Ricci, S., Ronchitelli, A., Valentin, F., Thevenet, C., Wehrberger, K., Grigorescu, D., Rougier, H., Crevecoeur, I., Flas, D., Semal, P., Mannino, M.A., Cupillard, C., Bocherens, H., Conard, N.J., Harvati, K., Moiseyev, V., Drucker, D.G., Svoboda, J., Richards, M.P., Caramelli, D., Pinhasi, R., Kelso, J., Patterson, N., Krause, J., Pääbo, S., Reich, D., 2016. The genetic history of ice age Europe. Nature 534, 200–205.

Gamble, C., Davies, W., Pettitt, P., Hazelwood, L., Richards, M., 2005. The archaeological and genetic foundations of the European population during the late-glacial: Implications for "Agricultural Thinking." Camb. Archaeol. J. 15, 193–223.

Gamble, C., Davies, W., Pettitt, P., Richards, M., 2004. Climate change and evolving human diversity in Europe during the last glacial. Philos. Trans. R. Soc. Lond. B Biol. Sci. 359, 243–253 discussion 253–4.

Ghinassi, M., Colonese, A.C., Di Giuseppe, Z., Govoni, L., Vetro, D.L., Malavasi, G., Martini, F., Ricciardi, S., Sala, B., 2009. The late pleistocene clastic deposits in the Romito Cave, southern Italy: a proxy record of environmental changes and human presence. J. Quat. Sci. 24 (4), 383–398.

Giraudi, C., 1989. Lake levels and climate for the last 30,000 years in the fucino area (Abruzzo-Central Italy) — a review. Palaeogeogr. Palaeoclimatol. Palaeoecol. 70, 249–260.

Graziosi, P., 1962. Découverte de gravures rupestres de type paléolithique dans l'abri du Romito (Italie). L'Anthropologie 66, 262–268.

Graziosi, P., 1971. Derniéres découvertes de gravures paléolithiques dans la grotte du Romito en Calabre. In: Mélanges André Varagnac, Paris, pp. 355–357.

Heyman, B.M., Heyman, J., Fickert, T., Harbor, J.M., 2013/1. Paleo-climate of the central European uplands during the last glacial maximum based on glacier mass-balance modeling. Quat. Res. 79, 49–54.

Higgs, E.S., Jarman, M.R., 1975. Palaeoeconomy. In: Higgs, H.S. (Ed.), Palaeoeconomy. Cambridge University Press, Cambridge, pp. 1–8.

Higham, T.F.G., Jacobi, R.M., Bronk Ramsey, C., 2006. AMS radiocarbon dating of ancient bone using ultrafiltration. Radiocarbon 48, 179–195.

Higham, T.F.G., Brock, F., Peresani, M., Broglio, A., Wood, R., Douka, K., 2009. Problems with radiocarbon dating the middle to upper palaeolithic transition in Italy. Quat. Sci. Rev. 28, 1257–1267.

Housley, R.A., Gamble, C.S., Street, M., Pettitt, P., 1997. Radiocarbon evidence for the lateglacial human recolonisation of northern Europe. Proc. Prehist. Soc. 63, 25–54.

Hughes, P.D., Gibbard, P.L., Ehlers, J., 2013. Timing of glaciation during the last glacial cycle: evaluating the concept of a global 'Last Glacial Maximum' (LGM). Earth Sci. Rev. 125, 171–198. https://doi.org/10.1016/j.earscirev.2013.07.003.

Huntley, B., Watts, W.A., Allen, J.R.M., Zolitschka, B., 1999. Palaeoclimate, chronology

and vegetation history of the Weichselian Lateglacial: comparative analysis of data from three cores at Lago Grande di Monticchio, southern Italy. Quat. Sci. Rev. 18, 945–960.
Jacobi, R.M., Higham, T.F.G., 2009. The early Lateglacial re-colonization of Britain: new radiocarbon evidence from Gough's cave, southwest England. Quat. Sci. Rev. 28, 1895–1913.
Lane, C.S., Blockley, S.P.E., Lotter, A.F., Bronk Ramsey, C., 2011. Tephrochronology and absolute centennial scale synchronisation of European and Greenland records for the last glacial to interglacial transition: a case study of Soppensee and NGRIP. Quat. Int. 246, 145–156.
López-García, J.M., Berto, C., Colamussi, V., Dalla Valle, C., Lo Vetro, D., Luzi, E., Malavasi, G., Martini, F., Sala, B., 2014. Palaeoenvironmental and palaeoclimatic reconstruction of the latest Pleistocene–Holocene sequence from Grotta del Romito (Calabria, southern Italy) using the small-mammal assemblages. Palaeogeogr. Palaeoclimatol. Palaeoecol. 409, 169–179.
Lo Vetro, D., Martini, F., 2016. Mesolithic in central-Southern Italy: overview of lithic productions. Quat. Int. 423, 279–302. https://doi.org/10.1016/j.quaint.2015.12.043.
Lowe, J.J., Hoek, W., INTIMATE Group, 2001. Inter-regional correlation of palaeoclimatic records for the Last Glacial-Interglacial Transition: a protocol for improved precision recommended by the INTIMATE project group. Quat. Sci. Rev. 20, 1175–1187.
Lowe, J.J., Barton, N., Blockley, S.P.E., Bronk Ramsey, C., Cullen, V., Davies, W., Gamble, C., Grant, K., Hardiman, M., Housley, R., Lane, C.S., Lee, S., Lewis, M., MacLeod, A., Menzies, M., Müller, W., Pollard, M., Price, C., Roberts, A.P., Rohling, E.J., Satow, C., Smith, V.C., Stringer, C.B., Tomlinson, E.L., White, D., Albert, P., Arienzo, I., Barker, G., Boric, D., Carandente, A., Civetta, L., Ferrier, C., Gaudelli, J.-L., Karkanas, P., Koumouzelis, M., Muller, U.C., Orsi, G., Pross, J., Rosi, M., Shalamanov-Korobar, L., Sirakov, N., Tzedakis, P.C., 2012. Volcanic ash layers illuminate the resilience of Neanderthals and early modern humans to natural hazards. Proc. Natl. Acad. Sci. U. S. A. 109, 13532–13537.
Martini, F., 2002. Grotta del Romito: Guide del Museo e Istituto Fiorentino di Preistoria. Museo e Istituto Fiorentino di Preistoria, Florence.
Martini, F., 2006. Le evidenze funerarie nella grotta e nel Riparo del Romito (Papasidero, Cosenza). In: Martini, F. (Ed.), La cultura del Morire nelle società preistoriche e protostoriche italiane. Studio interdisciplinare dei dati e loro trattamento informatico. Origines, Progetti, 3, Firenze, pp. 58–66.
Martini, F., Lo Vetro, D., 2005a. Grotta del Romito (Papasidero, Cosenza): recenti risultati degli scavi e degli studi. In: Ambrogio, B., Tiné, V. (Eds.), Atti delle giornate di studio sulla Preistoria e Protostoria della Calabria: Scavi e Ricerche 2003 Atti delle giornate di studio, Pellaro (RC), pp. 5–15.
Martini, F., Lo Vetro, D., 2005b. Il passaggio Gravettiano-Epigravettiano a Grotta del Romito (scavi 2003-2004). Prime osservazioni. In: Martini, F. (Ed.), Askategi, miscellanea in memoria di Georges Lapace, Rivista di Scienze Preistoriche LV, supplemento 1, Firenze, pp. 151–175.
Martini, F., Lo Vetro, D., 2007. Grotta del Romito (Papasidero, Prov. Di Cosenza). Riv. Sci. Preistoriche 57, 441–442.
Martini, F., Lo Vetro, D. (Eds.), 2011. Grotta del Romito a Papasidero: uomo, ambiente e cultura nel Paleolitico della Calabria: ricerche 1961-2011. Guide del Museo e Istituto fiorentino di Preistoria, Firenze. Editoriale Progetto 2000, Cosenza, 43-53.
Martini, F., Martino, G., Rolle, R., 2003. L'Epigravettiano finale di Grotta del Romito a Papasidero: L'industria litica degli strati C e D. Rev. Sci. Preistoricha 53, 55–138.
Martini, F., Cilli, C., Colonese, A.C., Di Giuseppe, Z., Ghinassi, M., Govoni, L., Lo Vetro, D., Martino, G., Ricciardi, S., 2007. L'Epigravettiano tra 15.000 e 10.000 anni da oggi nel basso versante tirrenico: casi studio dell'area calabro-campana. In: Martini, F. (Ed.), L'Italia tra 15.000 e 10.000 anni fa. Cosmopolitismo e regionalità nel Tardoglaciale, vol. 18. Atti della tavola rotonda, Florence, pp. 157–207.
Martini, F., Lo Vetro, D., Di Giuseppe, Z., Baglioni, L., Colonese, A.C., Lemorini, C., Mazzucco, N., Trenti, F., 2012. Strutture e sottostrutture del Paleolitico superiore di Grotta del Romito tra funzionalità e simbolismo. Rivista di Scienze Preistoriche, LXII, 33–66.
Martini, F., Lo Vetro, D., Dini, M., 2015. Prime osservazioni sul Gravettiano di Grotta del Romito: la produzione litica dell'orizzonte H4. In: Rinaldi, R., Romiti, E., Tozzi, C. (Eds.), Giornate in ricordo di Mario Dini, Rivista di Archeologia Storia Costume, anno XLIII - n. 1–2/2015. Istituto Storico Lucchese, Sezione delle Seimiglia, pp. 119–134.
Martini, F., Lo Vetro, D., Timpanelli, L., 2016. New insight on the Romito Shelter (Calabria): the lithic production of the mesolithic levels. In: Fontana, F., Visentin, D., Wierer, U. (Eds.), Proceedings of the MesoLife Conference, Selva di Cadore, 11th-14th June 2014, Preistoria Alpina, vol. 48, pp. 233–238.
Matthews, I.P., Trincardi, F., Lowe, J.J., Bourne, A.J., MacLeod, A., Abbott, P., Andersen, Asioli, A., Blockley, S.P.E., Lane, C.S., Oh, Y.A., Satow, C., Staff, R.A., Wulf, S., 2015. Developing a robust tephrochronological framework for late quaternary marine records in the Southern Adriatic Sea: new data from core station SA03-11. Quat. Sci. Rev. 118, 84–104.
Orsi, G., de Vita, S., Di Vito, M.A., 1996. The restless, resurgent Campi Flegrei nested caldera (Italy): constraints on its evolution and configuration. J. Volcanol. Geotherm. Res. 74, 179–214.
Palma di Cesnola, A., 1993. Il Paleolitico Superiore in Italia. Introduzione allo studio, Firenze.
Pellegrini, M., Donahue, R.E., Chenery, C., Evans, J., Lee-Thorp, J.A., Montgomery, J., Mussi, M., 2008. Faunal migration in late-glacial central Italy: implications for human resource exploitation. Rapid Commun. Mass Spectrom. 22, 1714–1726.
Pettitt, P.B., Davies, W., Gamble, C.S., Richards, M.B., 2003. Palaeolithic radiocarbon chronology: quantifying our confidence beyond two half-lives. J. Archaeol. Sci. 30, 1685–1693.
Posth, C., Renaud, G., Mittnik, A., Drucker, D.G., Rougier, H., Cupillard, C., Valentin, F., Thevenet, C., Furtwängler, A., Wißing, C., Francken, M., Malina, M., Bolus, M., Lari, M., Gigli, E., Capecchi, G., Crevecoeur, I., Beauval, C., Flas, D., Germonpré, M., van der Plicht, J., Cottiaux, R., Gély, B., Ronchitelli, A., Wehrberger, K., Grigorescu, D., Svoboda, J., Semal, P., Caramelli, D., Bocherens, H., Harvati, K., Conard, N.J., Haak, W., Powell, A., Krause, J., 2016. Pleistocene mitochondrial genomes suggest a single major dispersal of non-Africans and a lateglacial population turnover in Europe. Curr. Biol. 26, 827–833.
Ramrath, A., Zolitschka, B., Wulf, S., Negendank, J.F.W., 1999. Late Pleistocene climatic variations as recorded in two Italian maar lakes (Lago di Mezzano, Lago Grande di Monticchio). Quat. Sci. Rev. 18, 977–992.
Rasmussen, S.O., Andersen, K.K., Svensson, A.M., Steffensen, J.P., Vinther, B.M., Clausen, H.B., Siggaard-Andersen, M.L., Johnsen, S.J., Larsen, L.B., Dahl-Jensen, D., Bigler, M., Röthlisberger, R., Fischer, H., Goto-Azuma, K., Hansson, M.E., Ruth, U., 2006. A new Greenland ice core chronology for the last glacial termination. J. Geophys. Res. D Atmos. 111, 18–28.
Rasmussen, S.O., Bigler, M., Blockley, S.P.E., Blunier, T., Buchardt, S.L., Clausen, H.B., Cvijanovic, I., Dahl-Jensen, D., Johnsen, S.J., Fischer, H., Gkinis, V., Guillevic, M., Hoek, W.Z., Lowe, J.J., Pedro, J., Popp, T., Seierstad, I.K., Steffensen, J.P., Svensson, A.M., Vallelonga, P., Vinther, B.M., Walker, M.J.C., Wheatley, J.J., Winstrup, M., 2014. A stratigraphic framework for naming and robust correlation of abrupt climatic changes during the last glacial period based on three synchronized Greenland ice core records. Quat. Sci. Rev. 106, 14–28.
Reimer, P.J., Bard, E., Bayliss, A., Beck, J.W., Blackwell, P.G., Bronk Ramsey, C., Grootes, P.M., Guilderson, T.P., Hafliidason, H., Hajdas, I., Hatte, C., Heaton, T.J., Homann, D.L., Hogg, A.G., Hughen, K.A., Kaiser, K.F., Kromer, B., Manning, S.W., Niu, M., Reimer, R.W., Richards, D.A., Scott, E.M., Southon, J.R., Staff, R.A., Turney, C.S.M., van der Plicht, J., 2013. IntCal13 and Marine13 radiocarbon age calibration curves 0-50,000 Years cal BP. Radiocarbon 55, 1869–1887.
Robinson, S.A., Black, S., Sellwood, B.W., Valdes, P.J., 2006. A review of palaeoclimates and palaeoenvironments in the Levant and Eastern Mediterranean from 25,000 to 5000 years BP: setting the environmental background for the evolution of human civilisation. Quat. Sci. Rev. 25, 1517–1541.
Rodríguez-Rey, M., Herrando-Pérez, S., Gillespie, R., Jacobs, Z., Saltré, F., Brook, B.W., Prideaux, G.J., Roberts, R.G., Cooper, A., Alroy, J., Miller, G.H., Bird, M.I., Johnson, C.N., Beeton, N.J., Turney, C.S., Bradshaw, C.J.A., 2015. Criteria for assessing the quality of middle pleistocene to holocene vertebrate fossil ages. Quat. Geochronol. 30, 69–79. https://doi.org/10.1016/j.quageo.2015.08.002.
Rohling, E.J., Mayewski, P.A., Abu-Zied, R.H., Casford, J.S.L., Hayes, A., 2002. Holocene atmosphere¯ocean interactions: records from Greenland and the Aegean Sea. Clim. Dyn. 18, 587–593.
Siani, G., Paterne, M., Michel, E., Sulpizio, R., Sbrana, A., Arnold, M., Haddad, G., 2001. Mediterranean sea-surface radiocarbon reservoir age changes since the last glacial maximum. Science 294, 1917–1920.
Siani, G., Sulpizio, R., Paterne, M., Sbrana, A., 2004. Tephrostratigraphy study for the last 18,000 14C years in a deep-sea sediment sequence for the South Adriatic. Quat. Sci. Rev. 23, 2485–2500.
Siani, G., Magny, M., Paterne, M., Debret, M., Fontugne, M., 2013. Paleohydrology reconstruction and Holocene climate variability in the South Adriatic sea. Clim. Past 9. https://doi.org/10.5194/cp-9-499-2013. C463 499-515.
Sommer, R.S., Nadachowski, A., 2006. Glacial refugia of mammals in Europe: evidence from fossil records. Mamm. Rev. 36, 251–265.
Stiner, M.C., Munro, N.D., Surovell, T.A., 2000. The tortoise and the hare: small-game use, the broad-spectrum revolution, and paleolithic demography. Curr. Anthropol. 41, 39–73.
Strandberg, G., Brandefelt, J., Kjellström, E., Smith, B., 2011. High-resolution regional simulation of last glacial maximum climate in Europe. Tellus A 63, 107–125.
Straus, L.G., 1991. Human geography of the late upper paleolithic in Western Europe: present state of the question. J. Anthropol. Res. 47, 259–278.
Straus, L.G., 2005. The upper paleolithic of Cantabrian Spain. Evol. Anthropol. 14, 145–158.
Tallavaara, M., Luoto, M., Korhonen, N., Järvinen, H., Seppä, H., 2015. Human population dynamics in Europe over the last glacial maximum. Proc. Natl. Acad. Sci. U. S. A. 112, 8232–8237.
Tomlinson, E.L., Arienzo, I., Wulf, S., Smith, V.C., Carandente, A., Civetta, L., Hardiman, M., Lane, C.S., Orsi, G., Rosi, M., Thirlwall, M., Muller, W., Menzies, M.A., 2012. Geochemistry of the plegraean fields (Italy) proximal Campi Flegrei sources for major mediterranean tephras (C-1, C-2, Y-3 & Y- 5). Geochim. Cosmochim. Acta 93, 102–128.
Tomlinson, E.L., Albert, P.G., Wulf, S., Brown, R.J., Smith, V.C., Keller, J., Orsi, G., Bourne, A.J., Menzies, M., 2014. Age and geochemistry of tephra layers from Ischia, Italy: constraints from proximal-distal correlations with Lago Grande di Monticchio. J. Volcanol. Geotherm. Res. 287, 22–39.
Tomlinson, E.L., Smith, V.C., Albert, P.G., Aydar, E., Civetta, L., Cioni, R., Çubukçu, E., Gertisser, R., Isaia, R., Menzies, M.A., Orsi, G., Rosi, M., Zanchetta, G., 2015. The major and trace element glass compositions of the productive mediterranean volcanic sources: tools for correlating distal tephra layers in and around Europe. Quat. Sci. Rev. 118, 48–66.
Torroni, A., Bandelt, H.J., Macaulay, V., Richards, M., Cruciani, F., Rengo, C., Martinez-Cabrera, V., Villems, R., Kivisild, T., Metspalu, E., Parik, J., Tolk, H.V., Tambets, K., Forster, P., Karger, B., Francalacci, P., Rudan, P., Janicijevic, B., Rickards, O., Savontaus, M.L., Huoponen, K., Laitinen, V., Koivumäki, S., Sykes, B., Hickey, E.,

Novelletto, A., Moral, P., Sellitto, D., Coppa, A., Al-Zaheri, N., Santachiara-Benerecetti, A.S., Semino, O., Scozzari, R., 2001. A signal, from human mtDNA, of postglacial recolonization in Europe. Am. J. Hum. Genet. 69, 844–852.
Tzedakis, P.C., 2005. Towards an understanding of the response of southern European vegetation to orbital and suborbital climate variability. Quat. Sci. Rev. 25, 1585–1599.
Willis, K.J., Whittaker, R.J., 2000. Perspectives: paleoecology. The refugial debate. Science 287, 1406–1407.
Woodward, J.C., Goldberg, P., 2001. The sedimentary records in Mediterranean rockshelters and caves: archives of environmental change. Geoarchaeology 16, 327–354.
Wulf, S., Kraml, M., Brauer, A., Keller, J., Negendank, J.F.W., 2004. Tephrochronology of the 100ka lacustrine sediment record of Lago Grande di Monticchio. Quat. Int. 122, 7–30.
Wulf, S., Kraml, M., Keller, J., 2008. Towards a detailed distal tephrostratigraphy in the Central Mediterranean: the last 20,000 yrs record of Lago Grande di Monticchio. J. Volcanol. Geotherm. Res. 177, 118–132.